Electronic Supplementary Material (ESI) for ChemComm.
This journal is © The Royal Society of Chemistry 2023

Non-covalent interactions reveal the protein chain δ conformation in a flexible single-residue model

Zeynab Imani, Venkateswara Rao Mundlapati, Valérie Brenner, Eric Gloaguen, Katia Le Barbu-Debus, Anne Zehnacker-Rentien, Sylvie Robin, David J. Aitken, Michel Mons

Table of Contents

S1. Synthesis

S1.1 General information: instrumentation and materials

Materials and methods. Compound **1** (Cbz-Attc-NHMe) was prepared as described previously.[1] Tetrahydrothiophen-3-one was purchased from ABCR; isobutyl chloroformate (IBCF) and N-(benzyloxycarbonyloxy)succinimide (CbzOSu) were purchased from Fluorochem; benzyl chloroformate (CbzCl), methyl mercaptoacetate and methyl 4-bromobutyrate were purchased from Acros; N-methylmorpholine (NMM), 40% aqueous methylamine and Dowex 50WX8 cation-exchange resin (H^+ form, 50-100 mesh) were purchased from Sigma-Aldrich. These reagents were used as supplied, except for NMM which was distilled (120 °C) from KOH. THF was distilled from sodium/benzophenone under argon. Dry MeOH was purchased from Acros. All other solvents were purchased from VWR Chemicals or Carlo Erba and used as received (abbreviation: PE = petroleum ether, boiling range 40–65 °C). Preparative chromatography was performed on silica gel columns (40-63 μm). Analytical thin-layer chromatography was carried out on commercial silica gel TLC plates of 0.25 mm thickness (Merck, Silica Gel $60F_{254}$); after elution, the plates were visualized by fluorescence at 254 nm then revealed using acidic *p*-anisaldehyde solution (5% in EtOH), ninhydrin solution (14 mM in EtOH), or $KMnO_4$ solution (7.5% in water). Retention factors (R_f) are given for such TLC analyses.

Standard compound characterization. Melting points were measured in open capillary tubes on a Büchi B-540 apparatus and are uncorrected. Routine ^1H and ^{13}C NMR spectra were recorded at the indicated temperature on Bruker spectrometers operating at 250, 360 or 400 MHz for ^1H and at 62.5, 90 or 100 MHz for ^{13}C. For ^1H NMR spectra, chemical shifts (δ) are reported in parts per million (ppm) using residual protonated solvent as the internal reference (δ = 7.26 ppm for $CDCl_3$, δ = 2.50 ppm for DMSO-d_6, δ = 4.79 ppm for D_2O). Splitting patterns for ^1H signals are designated as s (singlet), bs (broad singlet), d (doublet), dd (double doublet), ddd (double double doublet), dddd (double double double doublet), t (triplet), quint. (quintuplet) or m (multiplet); coupling constants (J) are reported in hertz. For ^{13}C NMR spectra, chemical shifts (δ) are reported in parts per million (ppm) using the deuterated solvent as the internal reference δ = 77.2 ppm for $CDCl_3$, δ = 39.5 ppm for DMSO-d_6). Routine Fourier-transform infrared (IR) spectra were recorded on a Perkin Elmer Spectrum Two spectrometer for neat samples—whether liquid or solid—using the ATR diamond accessory; maximum absorbances (ν) for significant bands are given in cm^{-1}. High-resolution mass spectrometry (HRMS) data were recorded on a Bruker MicroTOF-Q instrument using positive-mode electrospray ionization.

S1.2 Synthesis of Cbz-Atlc-NHMe, **2**

Compound **2** was synthesized in racemic form according to Scheme S1. The strategy was based on the conversion of the commercial ketone starting material into the free amino acid **II** via hydantoin **I**, by a Bucherer-Bergs reaction followed by hydrolysis, using minor modifications of literature procedures.[2-4] However, protection of the isolated amino acid **II** as the benzyl carbamate **III** was inefficient. We therefore adapted the procedure to perform a three-step transformation of hydantoin **I** into the target molecule **2** (via the non-purified intermediates **II**·HCl and **III**) in a satisfactory 79% overall yield.

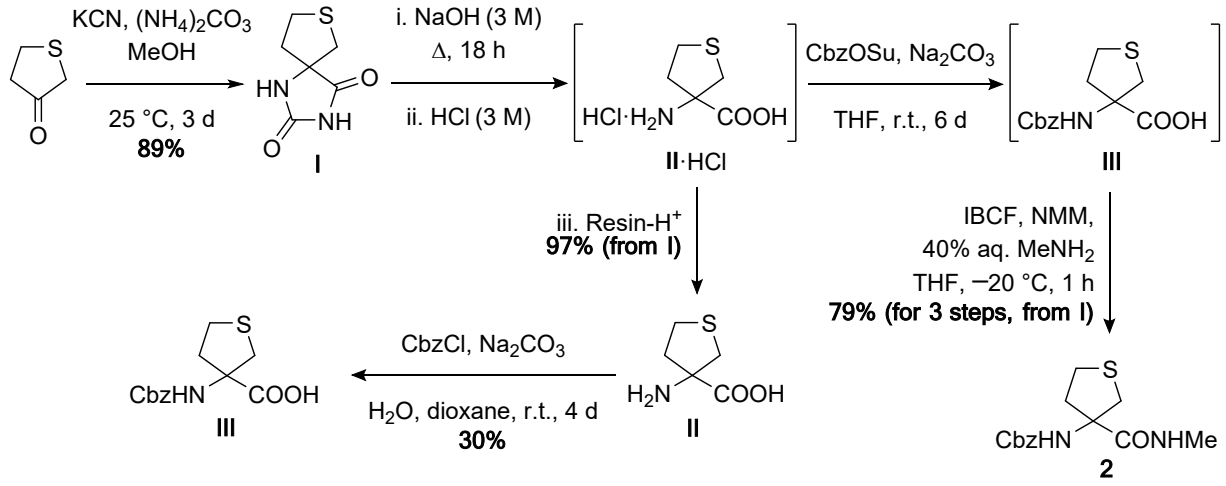

Scheme S1.

7-Thia-1,3-diazaspiro[4.4]nonane-2,4-dione, I. To a suspension of $(NH_4)_2CO_3$ (2.47 g, 25.7 mmol, 2.2 eq.) in MeOH (59 mL) in a 250 mL flask was added KCN (837 mg, 12.8 mmol, 1.1 eq.). The suspension was stirred for 30 min at 40 °C by which time a limpid solution was obtained. A solution of tetrahydrothiophen-3-one (1 mL, 11.7 mmol, 1 eq.) in MeOH (14 mL) was then added. The mixture was stirred for 30 min at 40 °C then for 3 d at 25 °C (temperature controlled with a water bath). The solvent was evaporated under reduced pressure and the residual sticky brown solid was treated with 6 M HCl to reach pH 1–2. The resulting light brown solid was recovered by filtration and was washed with a small amount of cold water to give the hydantoin **I** (1.80 g, 89%). This material was sufficiently pure for use directly in the next step without further purification.

To obtain an analytical sample, the product was recrystallized from H_2O:EtOH (3:1), after filtration of the hot solution to remove a dark brown polymer, to give the pure hydantoin **I** as light beige solid.

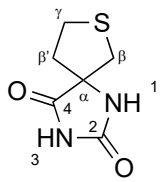

R_f = 0.68 (EtOAc:MeOH = 98:2).

Mp = 238–240 °C.

^{1}H NMR (360 MHz, DMSO-d_6, 300 K) δ 10.86 (s, 1H, NH^{1}), 8.47 (s, 1H, NH^{3}), 3.09 (d, ^{2}J = 12.3 Hz, 1H, $C^{\beta}H^{a}$), 3.05–2.93 (m, 2H, $C^{\gamma}H_2$), 3.09 (dd, ^{2}J = 12.3 Hz, ^{4}J = 0.9 Hz, 1H, $C^{\beta}H^{b}$), 2.19–2.00 (m, 2H, $C^{\beta'}H_2$).

^{13}C NMR (90 MHz, DMSO-d_6, 300 K) δ 175.9 ($C^{4}O$), 156.1 ($C^{2}O$), 70.5 (C^{α}), 40.3 ($C^{\beta'}H_2$), 39.6 ($C^{\beta}H_2$), 29.5 ($C^{\gamma}H_2$).

IR (neat) ν 3138, 3055, 2771, 1733 cm^{-1}.

HRMS [ESI(+)] *m/z* $[M+Na]^+$ calculated for $[C_6H_8N_2NaO_2S]^+$: 195.0199, found: 195.0202.

3-Aminothiolane-3-carboxylic acid (Atlc), II. A solution of **I** (3.63 g, 21.1 mmol, 1 eq.) in 3 M NaOH (77 mL, 11 eq.) was heated at reflux for 18 h in a 250 mL flask. After cooling, ammonia and water were removed under reduced pressure. The light-yellow residue was treated with 3 M HCl to reach pH 1–2. The resulting solution was applied to a column of cation-exchange resin (H^+ form) and eluted with 1 M NH_4OH solution give the amino acid **II** as a beige solid (3.00 g, 97%).

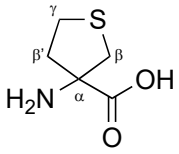

Mp = 199–202 °C.

^{1}H NMR (360 MHz, D_2O, 300 K) δ 3.30 (d, ^{2}J = 11.7 Hz, 1H, $C^{\beta}H^{a}$), 3.07 (ddd, ^{2}J = 11.1 Hz, ^{3}J = 8.2 Hz, ^{3}J = 2.9 Hz, 1H, $C^{\gamma}H^{a}$), 2.96 (ddd, ^{2}J = 10.9 Hz, ^{3}J = 10.3 Hz, ^{3}J = 6.5 Hz, 1H, $C^{\gamma}H^{b}$), 2.85 (dd, ^{2}J = 11.7 Hz, ^{4}J = 1.2 Hz, 1H, $C^{\beta}H^{b}$), 2.35 (ddd, ^{2}J = 13.4 Hz, ^{3}J = 10.1 Hz, ^{3}J = 8.3 Hz, 1H, $C^{\beta'}H^{a}$), 2.19 (dddd, ^{2}J = 13.4 Hz, ^{3}J = 6.2 Hz, ^{3}J = 2.9 Hz, ^{4}J = 1.3 Hz, 1H, $C^{\beta'}H^{b}$).

^{13}C NMR (100 MHz, D_2O, 300 K) δ 177.6 (CO acid), 69.2 (C^{α}), 40.4 ($C^{\beta}H_2$), 40.1 ($C^{\beta'}H_2$), 29.0 ($C^{\gamma}H_2$).

IR (neat) ν 2931, 1673, 1604, 1552, 1516 cm^{-1}.

HRMS [ESI(+)] *m/z* $[M+Na]^+$ calculated for $[C_5H_9NNaO_2S]^+$: 170.0246, found: 170.0246.

3-(Benzyloxycarbonylamino)thiolane-3-carboxylic acid, III. A suspension of Atlc **II** (1.00 g, 6.80 mmol, 1 eq.) in H_2O (30 mL) and dioxane (15 mL) was treated with Na_2CO_3 (2.162 g, 20.4 mmol, 4.5 eq.) and stirred until all the solid had dissolved. The solution was cooled to 0 °C and CbzCl (490 μL, 3.4 mmol, 0.5 eq.) was added dropwise; the solution was then stirred for 24 h at room temperature. The solution was cooled to 0 °C and more CbzCl was added dropwise (490 μL, 3.4 mmol, 0.5 eq.). This procedure was repeated two more times until a total of 2 eq. of CbzCl had been added to the solution. After a further 24 h at room temperature, the reaction mixture was concentrated to a volume of 10 mL under reduced

pressure. The residual solution was washed with hexane (3 × 30 mL) then slowly acidified at 0 °C with 2 M HCl until pH 1 was reached. The solution was then extracted with $CHCl_3$ (6 × 30 mL) and the combined organic layers were dried over $MgSO_4$, filtered and concentrated under reduced pressure. The purification was carried out by two successive chromatographies (CH_2Cl_2:MeOH:AcOH gradient 98:2:1 → 90:10:1) to give **Cbz-Atlc III** as a pale yellow solid (553 mg, 30%).

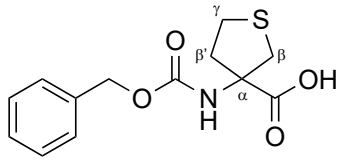

R_f = 0.28 (CH_2Cl_2:MeOH:AcOH = 95:5:1).

Mp = 153–155 °C.

^{1}H NMR (400 MHz, $CDCl_3$, 300 K) δ 8.04 (bs, 1H, OH), 7.45 – 7.18 (m, 5H, CH^{Ar}), 5.34 (bs, 1H, NH), 5.13 (s, 2H, $C^{Cbz}H_2$), 3.37 (d, ^2J = 11.8 Hz, 1H, $C^{\beta}H^a$), 3.04 (d, ^2J = 11.8 Hz, 1H, $C^{\beta}H^b$), 3.06–2.98 (m, 1H, $C^{\gamma}H^a$), 2.96–2.83 (m, 1H, $C^{\gamma}H^b$), 2.73–2.54 (m, 1H, $C^{\beta'}H^a$), 2.50–2.36 (m, 1H, $C^{\beta'}H^b$).

^{13}C NMR (100 MHz, $CDCl_3$, 300 K) δ 175.3 (CO acid), 156.0 (CO carbamate), 135.9 (C^{Ar}), 128.7, 128.5, 128.3 ($C^{Ar}H$), 68.4 (C^{α}), 67.6 ($C^{Cbz}H_2$), 39.8 ($C^{\beta}H_2$), 38.6 ($C^{\beta'}H_2$), 29.0 ($C^{\gamma}H_2$).

IR (neat) ν 3384, 2925, 1739, 1667, 1529 cm^{-1}.

HRMS [ESI(+)] *m/z* $[M+Na]^+$ calculated for $[C_{13}H_{15}NNaO_4S]^+$: 304.0614, found: 304.0608.

Benzyl 3-(methylcarbamoyl)thiolane-3-ylcarbamate, Cbz-Atlc-NHMe 2. A solution of **I** (667 mg, 3.88 mmol, 1 eq.) in 3 M NaOH (14 mL, 11 eq.) was heated at reflux for 18 h in a 25 mL flask. After cooling, ammonia and water were removed under reduced pressure. The light-yellow residue was treated with 3 M HCl to reach pH 1–2. The solution was evaporated to dryness under reduced pressure. The resulting sample of **II**·HCl was used directly in the next step.
To a solution of this **II**·HCl sample in a H_2O:THF (1:1) mixture (42 mL) in an argon-flushed flask was added Cbz-OSu (1.45 g, 5.83 mmol, 1.62 eq.) then Na_2CO_3 (501 mg, 4.73 mmol, 1.31 eq.). The resulting solution was stirred for 5 d at room temperature. THF was then removed under reduce pressure. The aqueous layer was washed with hexane (3 × 20 mL) and acidified slowly at 0 °C by addition of 2 M HCl to reach pH 1. The aqueous layer was extracted with EtOAc (6 × 20 mL). The combined organic layers were dried over $MgSO_4$, filtered and concentrated under reduce pressure. Purification was carried out by chromatography (CH_2Cl_2:MeOH:AcOH gradient 98:2:1 → 90:10:1) to give crude **Cbz-Atlc III** as a dark yellow oil.

To a cold (–20 °C) solution of this crude **Cbz-Atlc III** in THF (7 mL) in an argon-flushed 25 mL flask were added successively NMM (411 μL, 3.7 mmol, 1 eq.) and IBCF (495 μL, 3.7 mmol, 1 eq.). The activation period was 10 min. A solution of 40% aq. $MeNH_2$ (3 mL, 34.00 mmol, 10 eq.) in THF (3 mL) was then added and the solution was stirred for 1 h 30 at –20 °C, followed by addition of 5% aq. $NaHCO_3$ (5 mL). The resulting mixture was stirred for 1 h at room temperature, then extracted with CH_2Cl_2 (6 × 20 mL). The combined organic layers were washed with 5% aq. $NaHCO_3$ (2 × 5 mL), dried over $MgSO_4$, filtered and concentrated under reduced pressure. The residue was purified by flash chromatography (PE:EtOAc gradient 7:3 → 0:1) to give **Cbz-Atlc-NHMe 2** as a light yellow solid (789 mg, 79%).

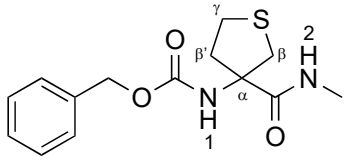

R_f = 0.62 (EtOAc).

Mp = 144–145 °C.

^{1}H NMR (360 MHz, $CDCl_3$, 300 K) δ 7.44–7.29 (m, 5H, CH^{Ar}), 6.81 (bs, 1H, NH^2), 5.45 (bs, 1H, NH^1), 5.11 (s, 2H, $C^{Cbz}H_2$), 3.27 (d, ^2J = 11.9 Hz, 1H, $C^{\beta}H^b$), 3.13-2.99 (m, 1H, $C^{\beta}H^a$), 3.02–2.93 (m, 1H, $C^{\gamma}H^b$), 2.93–2.83 (m, 1H, $C^{\gamma}H^a$), 2.86 (d, ^3J = 4.5 Hz, 3H, NCH_3), 2.68–2.53 (m, 1H, $C^{\beta'}H^a$), 2.52–2.36 (m, 1H, $C^{\beta'}H^b$).

^{13}C NMR (100 MHz, $CDCl_3$, 300 K) δ 171.7 (CO amide), 155.5 (CO carbamate), 136.0 (C^{Ar}), 128.8, 128.5, 128.3 ($C^{Ar}H$), 69.3 (C^{α}), 67.3 ($C^{Cbz}H_2$), 39.8 ($C^{\beta}H_2$), 38.0 ($C^{\beta'}H_2$), 28.8 ($C^{\gamma}H_2$), 26.8 (NCH_3).

IR (neat) ν 3316, 3061, 2937, 1693, 1648, 1518 cm^{-1}.

HRMS [ESI(+)] *m/z* $[M+Na]^+$ calculated for $[C_{14}H_{18}N_2NaO_3S]^+$: 317.0930, found: 317.0921.

S1.3 Synthesis of Cbz-Atc-NHMe, **3**

Compound **3** was synthesized in racemic form according to Scheme S2. The intermediate cyclic ketone **VI** was prepared using minor adaptations of the literature precedents.[5-7] The amino acid **VIII** has been mentioned in the literature but without preparative details.[8-10] Our strategy was to prepare it via the intermediate hydantoin **VII**, based on literature describing the conversion of other thiacyclic ketones into amino acids. [2-4, 11] and on the synthesis of compound **2** described above (Section S1.2).

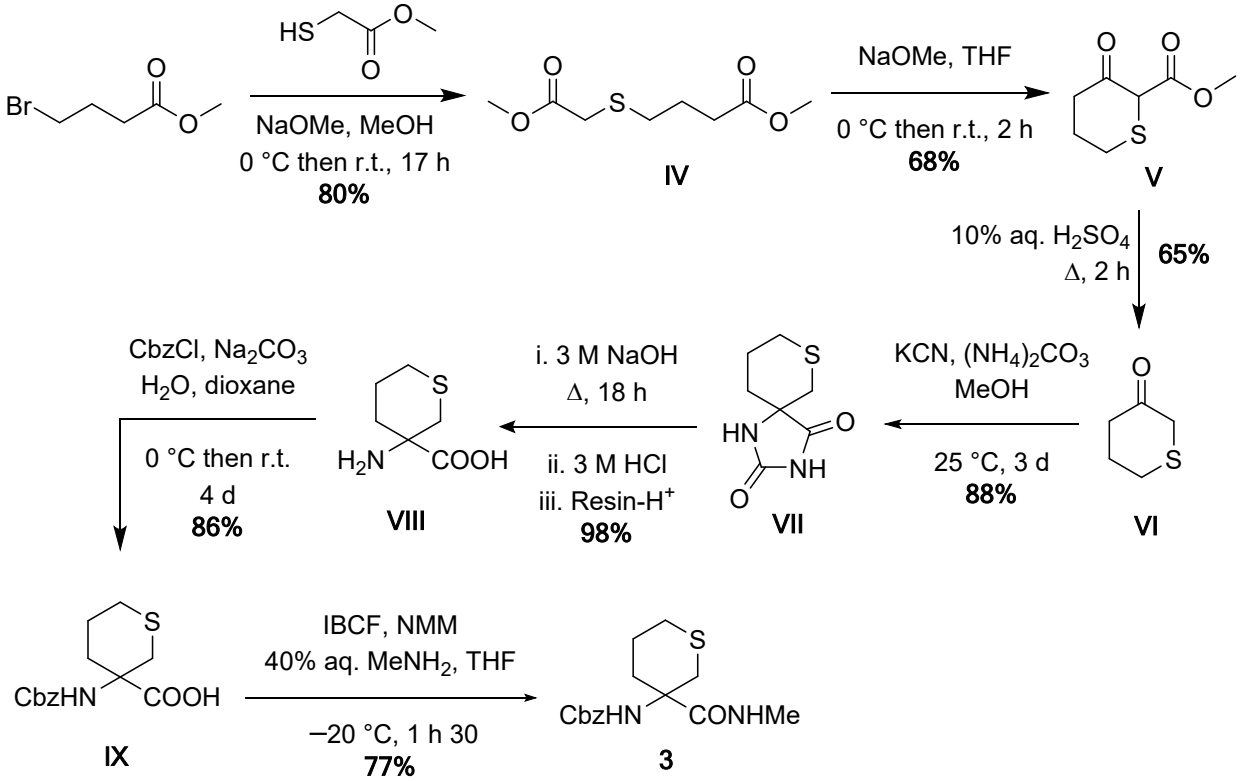

Scheme S2.

Methyl 4-(2-methoxy-2-oxoethylthio)butanoate, IV. Small portions of sodium metal (2.30 g, 100 mmol, 1 eq.) were added cautiously to dry MeOH (50 mL) at 0 °C in an argon-flushed two-necked flask. The mixture was stirred until a solution was obtained. Methyl mercaptoacetate (9.0 mL, 100 mmol, 1 eq.) was added slowly followed by slow addition of methyl 4-bromobutyrate (12.6 mL, 100 mmol, 1 eq.). The resulting mixture was stirred for 17 h whilst returning to room temperature. The precipitate (NaBr) was filtered off and washed with MeOH and the filtrate was concentrated under reduce pressure. The viscous residue was digested with water (50 mL) and extracted with Et_2O (6 × 50 mL). The combined organic layers were dried over $MgSO_4$, filtered and evaporated under reduced pressure. The residue was purified by flash chromatography (PE:EtOAc gradient 1:0 → 5:5 → 0:1) to give the diester **IV** as a colorless oil (16.6 g, 80%).

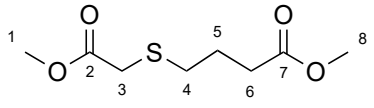

R_f = 0.57 (PE:Et_2O = 1:1).

^{1}H NMR (360 MHz, $CDCl_3$, 300 K) δ 3.74 (s, 3H, C^1H_3), 3.68 (s, 3H, C^8H_3), 3.22 (s, 2H, C^3H_2), 2.68 (t, ^3J = 7.2 Hz, 2H, C^4H_2), 2.44 (t, ^3J = 7.3 Hz, 2H, C^6H_2), 1.90 (quint., ^3J = 7.3 Hz, 2H, C^5H_2).

^{13}C NMR (90 MHz, $CDCl_3$, 300 K) δ 173.5 (C^7O ester), 171.0 (C^2O ester), 52.5 (C^1H_3), 51.8 (C^8H_3), 33.3 (C^3H_2), 32.7 (C^6H_2), 32.0 (C^4H_2), 24.1 (C^5H_2).

IR (neat) ν 2953, 1729 cm^{-1}.

HRMS [ESI(+)] *m/z* $[M+Na]^+$ calculated for $[C_8H_{14}NaO_4S]^+$: 229.0505, found: 229.0507.

Methyl 3-oxotetrahydro-2*H*-thiopyran-2-carboxylate, V. To an ice-cooled suspension of finely chopped sodium metal (2.12 g, 92.4 mmol, 0.95 eq.) in THF (134 mL) in an argon-flushed two-necked flask was added dropwise dry MeOH (3.93 mL, 97.2 mmol, 1.0 eq.). The suspension was stirred for 24 h and allowed to rise to room temperature, during which time a fine white suspension of NaOMe appeared. The suspension was cooled to 0 °C and diester **IV** (14.6 g, 70.8 mmol, 0.73 eq.) was added dropwise by syringe; the latter was rinsed with THF (7 mL) which was added to the mixture. The resulting amber solution was stirred for 2 h at room temperature then transferred to a 1 L beaker and cooled to 0 °C with stirring while 50% aq. H_2SO_4 (47.6 mmol, 0.49 eq.) was added slowly; the temperature was kept below 20 °C (ice bath). To the resulting light-yellow mixture was added CH_2Cl_2 (71 mL) which caused the formation of a precipitate. Solid Na_2SO_4 (197 mg) and $NaHCO_3$ (201 mg) were added and the suspension was stirred for a further 45 min. The mixture was filtered and the yellow solid residue was washed with CH_2Cl_2 (25 mL). The combined bright yellow filtrate and washings were evaporated under reduced pressure. The resulting crude product was purified by vacuum distillation, collecting the fraction bp = 85–87 °C (15 mbar), to give the keto ester **V** as a colorless oil (8.42 g, 68%).
Spectroscopic analysis showed that the product existed largely as its enol form (keto:enol 1:4).

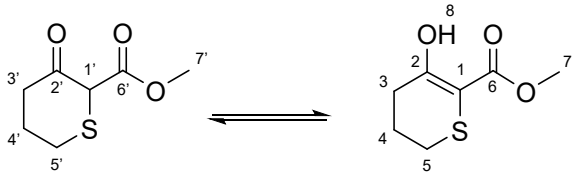

keto form enol form

R_f = 0.76 (PE:Et_2O = 1:1).

^{1}H NMR (250 MHz, $CDCl_3$, 300 K) δ *enol form:* 12.17 (s, 1H, OH), 3.81 (s, 3H, C^7H_3), 2.86–2.73 (m, 2H, C^5H_2), 2.50–2.34 (m, 2H, C^3H_2), 2.21–2.05 (m, 2H, C^4H_2); *keto form:* 3.99 (s, 1H, $C^{1'}H$), 3.80 (s, 3H, $C^{7'}H_3$), 3.15–3.01 (m, 2H, $C^{5'}H_2$), 2.71–2.57 (m, 2H, $C^{3'}H_2$), 2.49–2.34 (m, 2H, $C^{4'}H_2$).

^{13}C NMR (62.5 MHz, $CDCl_3$, 300 K) *δ enol form:* 170.6 (C^2), 167.2 (C^6), 93.5 (C^1), 52.4 (C^7H_3), 28.9 (C^3H_2), 26.9 (C^5H_2), 24.3 (C^4H_2); *keto form:* 199.8 ($C^{2'}$), 168.2 ($C^{6'}$), 56.4 ($C^{1'}$), 53.2 ($C^{7'}H_3$), 40.4 ($C^{3'}H_2$), 33.6 (C^5H_2), 26.7 ($C^{4'}H_2$).

IR (neat) *v* 3199 (br), 2953, 1729, 1705, 1581 cm^{-1}.

Dihydro-2*H*-thiopyran-3(4*H*)-one, VI. A solution of 10% aq. H_2SO_4 (70.3 mL, 12.9 mmol, 0.3 eq.) in a two-necked flask equipped with a condenser was heated under reflux, while keto ester **V** (6.95 g, 40 mmol, 1 eq.) was added dropwise. The resulting suspension was stirred vigorously for 1.5 h under reflux. After cooling at room temperature, the mixture was extracted with CH_2Cl_2 (8 × 50 mL). Combined organic layers were dried over $MgSO_4$, filtered and evaporated under reduced pressure. The crude product was purified by vacuum distillation, collecting the fraction bp = 45–47 °C (0.4 mbar) to give the cyclic ketone **VI** as a colorless oil (3.04 g, 65%).

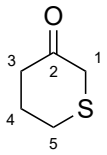

***R*$_f$** = 0.18 (PE:Et_2O = 9:1).

^{1}H NMR (400 MHz, $CDCl_3$, 300 K) *δ* 3.19 (s, 2H, C^1H_2), 2.81–2.71 (m, 2H, C^5H_2), 2.51–2.30 (m, 4H, C^3H_2 and C^4H_2).

^{13}C NMR (100 MHz, $CDCl_3$, 300 K) *δ* 204.0 (C^2O), 42.0 (C^3H_2), 38.8 (C^1H_2), 33.5 (C^4H_2), 28.7 (C^5H_2).

IR (neat) *v* 2919, 2857, 1702 cm^{-1}.

7-Thia-1,3-diazaspiro[4.5]decane-2,4-dione, VII. To a suspension of $(NH_4)_2CO_3$ (1.82 g, 18.9 mmol, 2.2 eq.) in MeOH (43 mL) in a 100 mL flask was added KCN (617 mg, 9.5 mmol, 1.1 eq.). The suspension was stirred for 30 min at 40 °C by which time a limpid solution was obtained. A solution of **VII** (1.00 g, 8.6 mmol, 1 eq.) in MeOH (11 mL) was then added. The mixture was stirred for 30 min at 40 °C then for 3 d at 25 °C (temperature controlled with a water bath). The solvent was evaporated under reduced pressure and the residual sticky brown solid was treated with 6 M HCl to reach pH 1–2. The resulting shiny white solid was recovered by filtration and was washed with a small amount of cold water to give the hydantoin **VII** (1.40 g, 88%). This material was used directly in the next step without further purification.

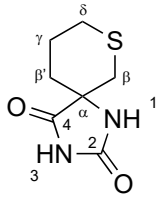

R_f = 0.70 (EtOAc:MeOH = 98:2).

Mp = 223–225 °C.

^{1}H NMR (360 MHz, DMSO-d_6, 300 K) δ 10.67 (bs, 1H, NH^1), 8.50 (bs, 1H, NH^3), 2.89 (d, ^2J = 13.5 Hz, 1H, $C^{\beta}H^a$), 2.71–2.56 (m, 1H, $C^{\delta}H^a$), 2.52–2.42 (m, 1H, $C^{\delta}H^b$), 2.51–2.43 (m, 1H, $C^{\beta}H^b$), 1.96–1.79 (m, 2H, $C^{\beta'}H^a$ + $C^{\gamma}H^a$), 1.78–1.64 (m, 1H, $C^{\gamma}H^b$), 1.63–1.52 (m, 1H, $C^{\beta'}H^b$).

^{13}C NMR (90 MHz, DMSO-d_6, 300 K) δ 177.1 (C^4O), 156.1 (C^2O), 60.2 (C^{α}), 34.3 ($C^{\beta}H_2$), 32.6 ($C^{\beta'}H_2$), 33.5 ($C^{\delta}H_2$), 28.7 ($C^{\gamma}H_2$).

IR (neat) ν 3181, 3059, 2937, 1769, 1709 cm^{-1}.

HRMS [ESI(+)] *m/z* $[M+Na]^+$ calculated for $[C_7H_{10}N_2NaO_2S]^+$: 209.0355, found: 209.0351.

3-Aminothiane-3-carboxylic acid (Atc), VIII. A solution of **VII** (600 mg, 3.22 mmol, 1 eq.) in 3 M NaOH (12 mL, 11 eq.) was heated at reflux for 18 h in a 10 mL flask. After cooling, ammonia and water were removed under reduced pressure. The light-yellow residue was treated with 3 M HCl (12 mL) to reach pH 1–2. The resulting solution was applied to a column of cation-exchange resin (H^+ form) and eluted with 1M NH_4OH solution give the amino acid **VIII** as a beige solid (509 mg, 98%).

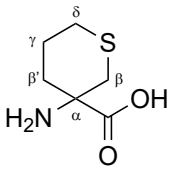

Mp = 261-263 °C.

^{1}H NMR (360 MHz, D_2O, 300 K) δ 3.27 (d, ^2J = 14.5 Hz, 1H, $C^{\beta}H^a$), 2.79–2.67 (m, 1H, $C^{\delta}H^a$), 2.71–2.61 (m, 1H, $C^{\beta}H^b$), 2.61–2.51 (m, 1H, $C^{\delta}H^b$), 2.09–1.90 (m, 2H, $C^{\beta'}H_2$), 2.07–1.97 (m, 1H, $C^{\gamma}H^a$), 1.83–1.69 (m, 1H, $C^{\gamma}H^b$).

^{13}C NMR (90 MHz, D_2O, 300 K) δ 175.6 (CO acid), 58.9 (C^{α}), 33.1 ($C^{\beta}H_2$), 30.9 ($C^{\beta'}H_2$), 27.0 ($C^{\delta}H_2$), 21.4 ($C^{\gamma}H_2$).

IR (neat) ν 3320, 3056, 3020, 2949, 2925, 1733 cm^{-1}.

HRMS [ESI(+)] *m/z* $[M+Na]^+$ calculated for $[C_6H_{11}NNaO_2S]^+$: 288.0301, found: 288.0297.

3-(Benzyloxycarbonylamino)thiane-3-carboxylic acid, IX. A suspension of **VIII** (200 mg, 1.24 mmol, 1.0 eq.) in H_2O (7 mL) and dioxane (5 mL) was treated with Na_2CO_3 (263 mg, 2.48 mmol, 2.0 eq.) and stirred until all the solid had dissolved. The solution was cooled to 0 °C and CbzCl (180 μL, 1.26 mmol,

1.0 eq.) was added dropwise; the solution was then stirred for 24 h at room temperature. The solution cooled to 0 °C and more CbzCl (90 μL, 0.63 mmol, 0.5 eq.) was added dropwise. After 6 h at room temperature, dioxane was removed under reduced pressure. The residual aqueous layer was washed with hexane (3 × 20 mL) then slowly acidified at 0 °C with 2 M HCl to reach pH 1. The aqueous layer was extracted with EtOAc (6 × 20 mL). The combined organic layers were dried over $MgSO_4$, filtered and concentrated under reduce pressure to give **Cbz-Atc IX** as a light yellow solid (316 mg, 86%).

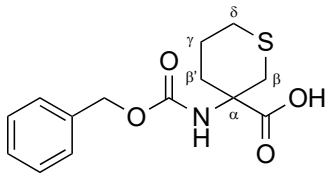

R_f = 0.36 (CH_2Cl_2:MeOH:AcOH = 95:5:1).

Mp = 141–144 °C.

^{1}H NMR (360 MHz, $CDCl_3$, 300 K) δ 8.60 (bs, 1H, OH), 7.45–7.28 (m, 5H, CH^{Ar}), 5.80 (bs, 1H, NH), 5.14 (s, 2H, $C^{Cbz}H_2$), 3.08 (d, ^2J = 13.8 Hz, 1H, $C^{\beta}H^a$), 2.81 (d, ^2J = 13.7 Hz, 1H, $C^{\beta}H^b$), 2.68–2.54 (m, 1H, $C^{\delta}H^a$), 2.51–2.41 (m, 1H, $C^{\delta}H^b$), 2.42–2.31 (m, 1H, $C^{\beta'}H^a$), 1.99–1.88 (m, 1H, $C^{\gamma}H^a$), 1.90–1.77 (m, 1H, $C^{\beta'}H^a$), 1.87–1.70 (m, 1H, $C^{\gamma}H^b$).

^{13}C NMR (90 MHz, $CDCl_3$, 300 K) δ 177.0 (CO acid), 155.6 (CO carbamate), 136.0 (C^{Ar}), 128.7, 128.4, 128.3 ($C^{Ar}H$), 67.5 ($C^{Cbz}H_2$), 56.4 (C^{α}), 35.5 ($C^{\beta}H_2$), 30.1 ($C^{\beta'}H_2$), 27.9 ($C^{\delta}H_2$), 22.4 ($C^{\gamma}H_2$).

IR (neat) ν 3314, 2928, 2895, 1713, 1518 cm^{-1}.

HRMS [ESI(+)] *m/z* $[M+Na]^+$ calculated for $[C_{14}H_{17}NNaO_2S]^+$: 318.0771, found: 318.0769.

Benzyl 3-(methylcarbamoyl)thiane-3-ylcarbamate, Cbz-Atc-NHMe 3. To a cold (– 20 °C) solution of **IX** (390 mg, 1.46 mmol, 1 eq.) in THF (6 mL) in an argon-flushed 25 mL flask were added successively NMM (176 μL, 1.60 mmol, 1 eq.) and IBCF (208 μL, 1.60 mmol, 1 eq.). The activation period was 10 min. A solution of 40% aq. $MeNH_2$ (1.3 mL, 14.6 mmol, 10 eq.) in THF (2 mL) was then added and the solution was stirred for 1.5 h at –20 °C, followed by addition of 5% aq. $NaHCO_3$ (5 mL). The resulting mixture was stirred for 1 h at room temperature then extracted with CH_2Cl_2 (6 × 20 mL). The combined organic layers were washed with 5% aq. $NaHCO_3$ (2 × 5 mL), dried over $MgSO_4$, filtered and concentrated under reduced pressure. The residue was purified by flash chromatography (PE:EtOAc gradient 7:3 → 0:1) to give **Cbz-Atc-NHMe 3** as a sticky cream solid (345 mg, 77%).

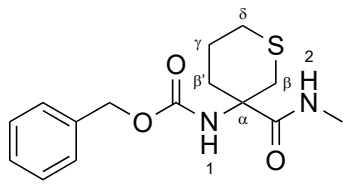

R_f = 0.35 (EtOAc).

Mp = 95–97 °C.

^{1}H NMR (400 MHz, $CDCl_3$, 300 K) δ 7.44–7.26 (m, 5H, CH^{Ar}), 6.71 (bs, 1H, NH^2), 5.75 (s, 1H, NH^1), 5.09 (s 2H, $C^{Cbz}H_2$), 3.11 (d, ^2J = 14.0 Hz, 1H, $C^{\beta}H^b$), 2.75 (bs, 3H, NCH_3), 2.74–2.62 (m, 1H, $C^{\beta}H^a$), 2.64–2.50 (m, 1H, $C^{\delta}H^{a/b}$), 2.46–2.35 (m, 1H, $C^{\delta}H^{a/b}$), 2.35–2.18 (m, 1H, $C^{\beta'}H^a$), 1.97–1.76 (m, 2H, $C^{\beta'}H^b$, $C^{\gamma}H^b$), 1.75–1.57 (m, 1H, $C^{\gamma}H^a$).

^{13}C NMR (100 MHz, $CDCl_3$, 300 K) δ 173.7 (CO amide), 155.3 (CO carbamate), 136.1 (C^{Ar}), 128.6, 128.3, 128.1 ($C^{Ar}H$), 67.0 ($C^{Cbz}H_2$), 56.9 (C^{α}), 35.7 ($C^{\beta}H_2$), 29.7 ($C^{\beta'}H_2$), 27.8 ($C^{\delta}H_2$), 26.5 (NCH_3), 22.6 ($C^{\gamma}H_2$).

IR (neat) ν 3320, 2945, 1724, 1692, 1655, 1521 cm^{-1}.

HRMS [ESI(+)] *m/z* $[M+Na]^+$ calculated for $[C_{15}H_{20}N_2NaO_3S]^+$: 331.1087, found: 331.1081.

S1.4 Copies of ^{1}H and ^{13}C NMR spectra of compounds **1**, **2** and **3**.

Cbz-Attc-NHMe 1

The NMR spectra of **1** are adapted from ref. 1 and are reproduced here for comparison.

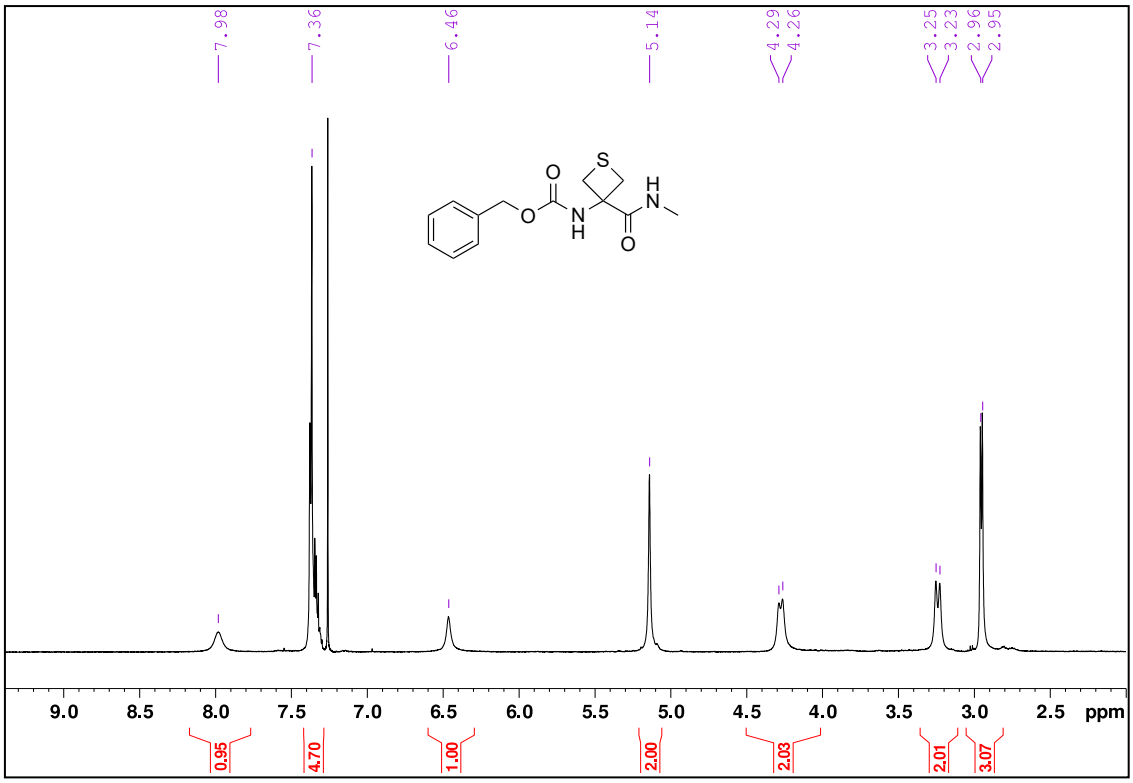

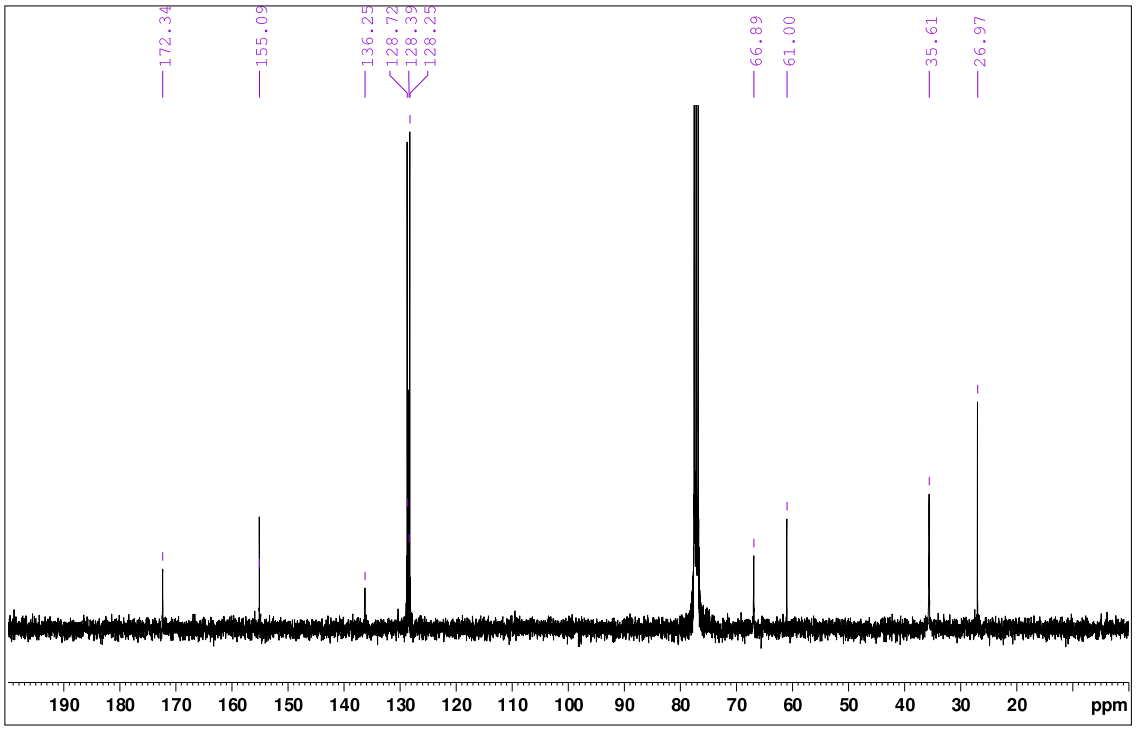

Cbz-Atlc-NHMe 2

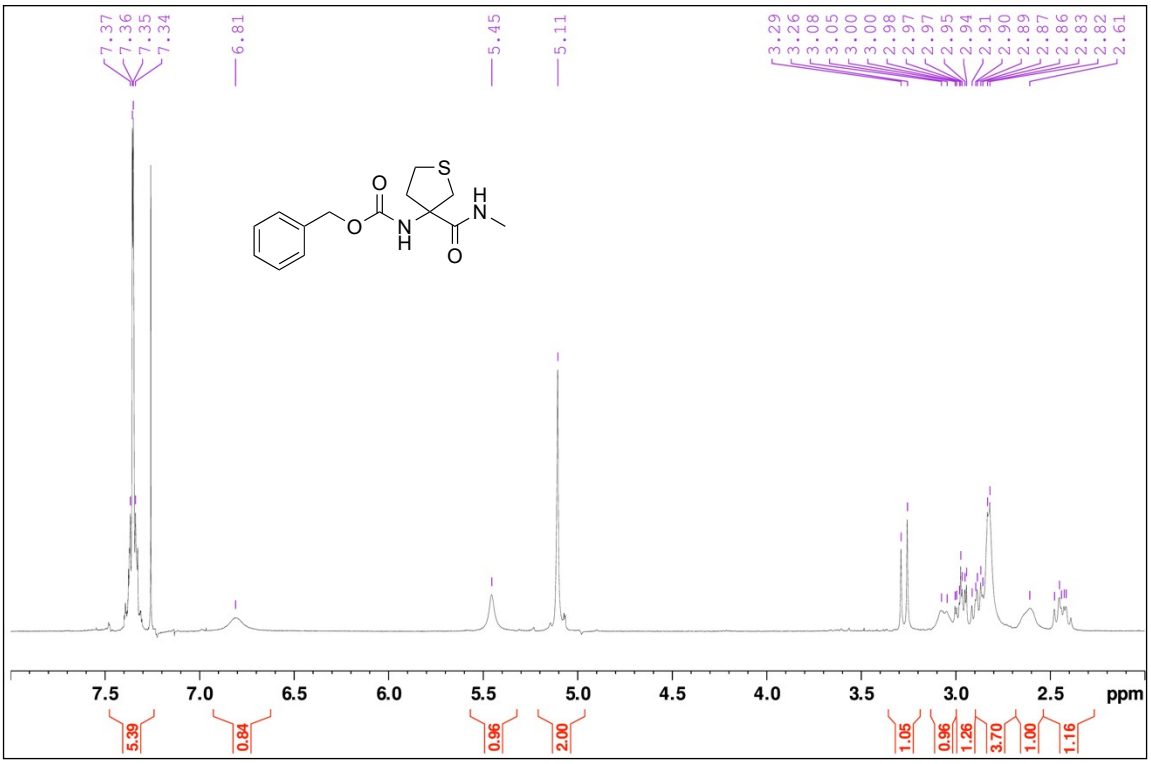

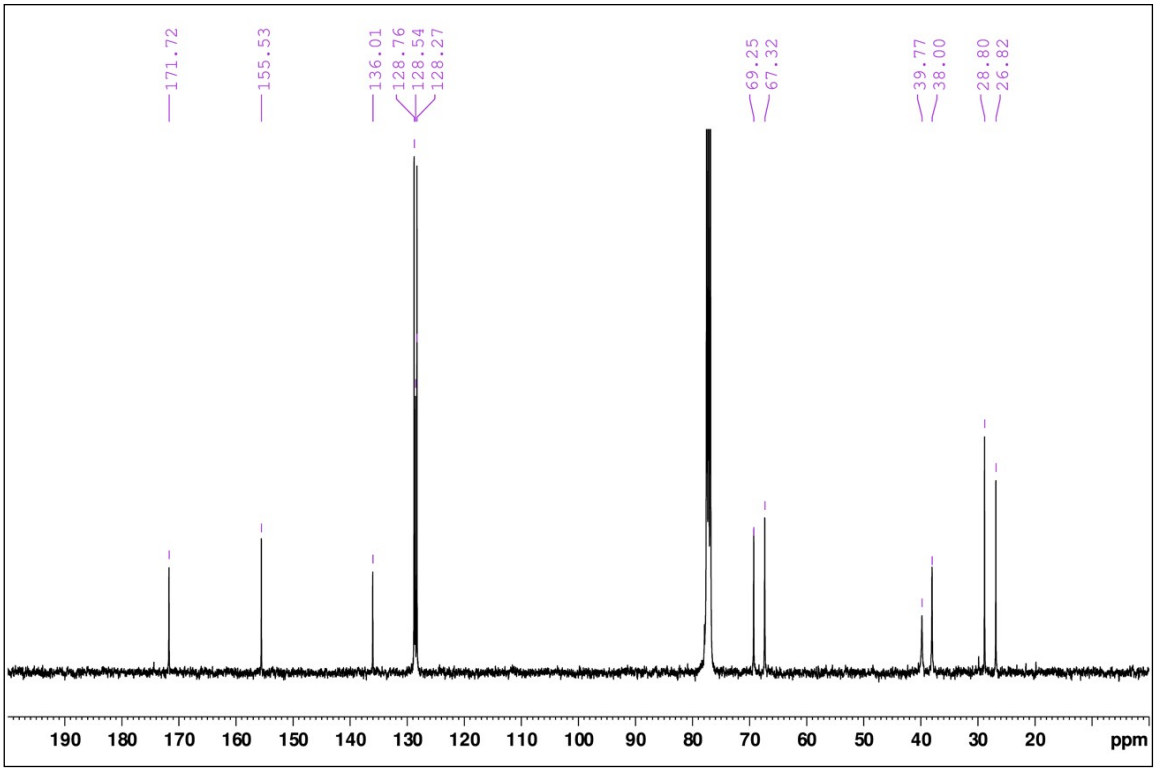

Cbz-Atc-NHMe 3

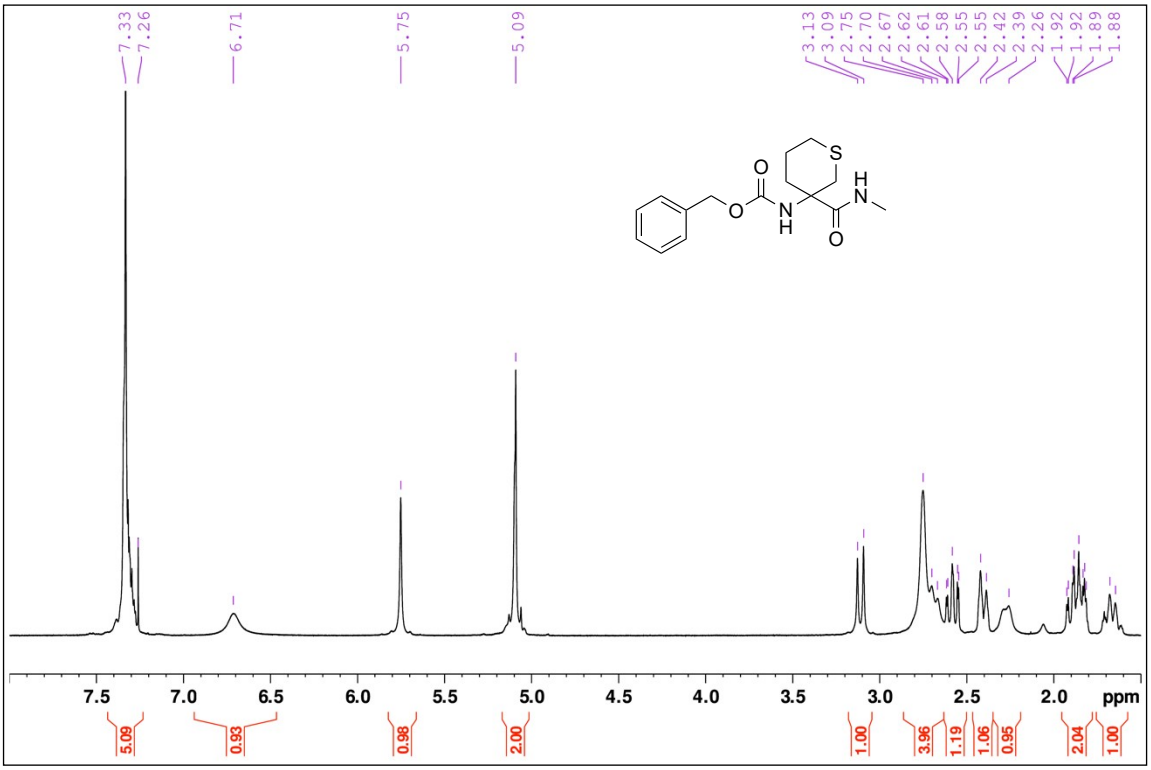

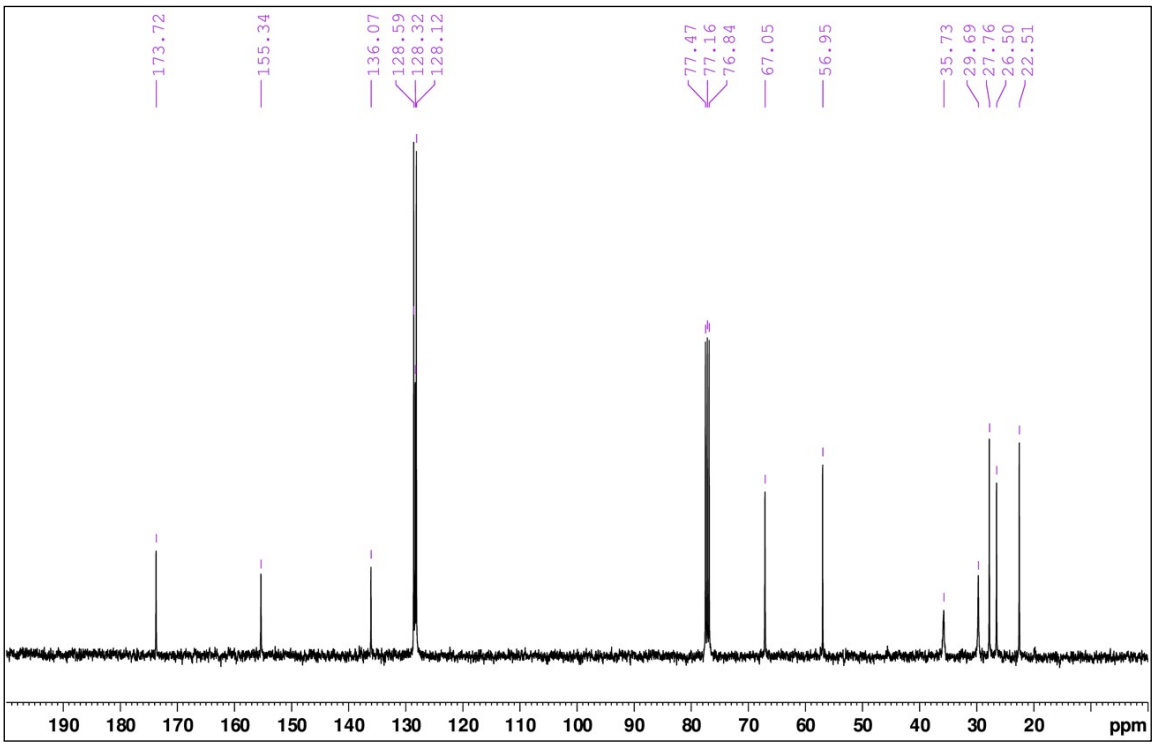

S2. Theoretical chemistry

S2.1 Methodology

A theoretical conformational analysis was first carried out using a force-field exploration using the MacroModel suite,[12] followed by a more precise quantum chemistry characterization, first in vacuo and then in solution using a standard continuous solvent approach, using the Turbomole package,[13] in order to get the relevant parameters for interpreting IR spectroscopy, namely energetics at both 0 K and 300 K and harmonic vibrational frequencies. Geometry optimizations were carried at the B97-D3 level of theory[14] using the Becke-Johnson damping and the three-body term options (B97-D3(BJ)-abc), with a def2-TZVPPD basis set.[15, 16] The resolution-of-identity (RI) approximation[17] and the auxiliary associated basis[18-20] were also used. A *m3* default grid size and a convergence threshold of 10^{-5} a.u. on the norm of the Cartesian gradient were used. Numerical harmonic frequencies were calculated at the same level of theory, using the *numforce* module with the *central* option and a step length of 0.02 a.u. This RI-B97-D3(BJ)-abc/def2-TZVPPD level already proved to be a good compromise between optimized structures, energetics, vibrational frequency and calculation times, in a context where dispersion interactions are ubiquitous.[1, 21] For a close comparison with experimental data, the harmonic frequencies were scaled according to a mode-dependent scaling procedure described in detail previously,[22] with, for the amide A, I and II regions, a scaling factor of 0.978, 1.008 and 1.004 respectively.

Structures, energetics and frequencies in solution were carried out using the Conductor-like Screening Model approximation (COSMO),[23] implemented in the Turbomole Package, where the solute molecule forms a cavity within the dielectric continuum of permittivity ε that represents the solvent. For chloroform, ε was taken as 4.81. For comparison with solution spectra in the NH stretch region, a fair agreement was found by scaling the harmonic frequencies by 0.9685.

S2.2 Structures

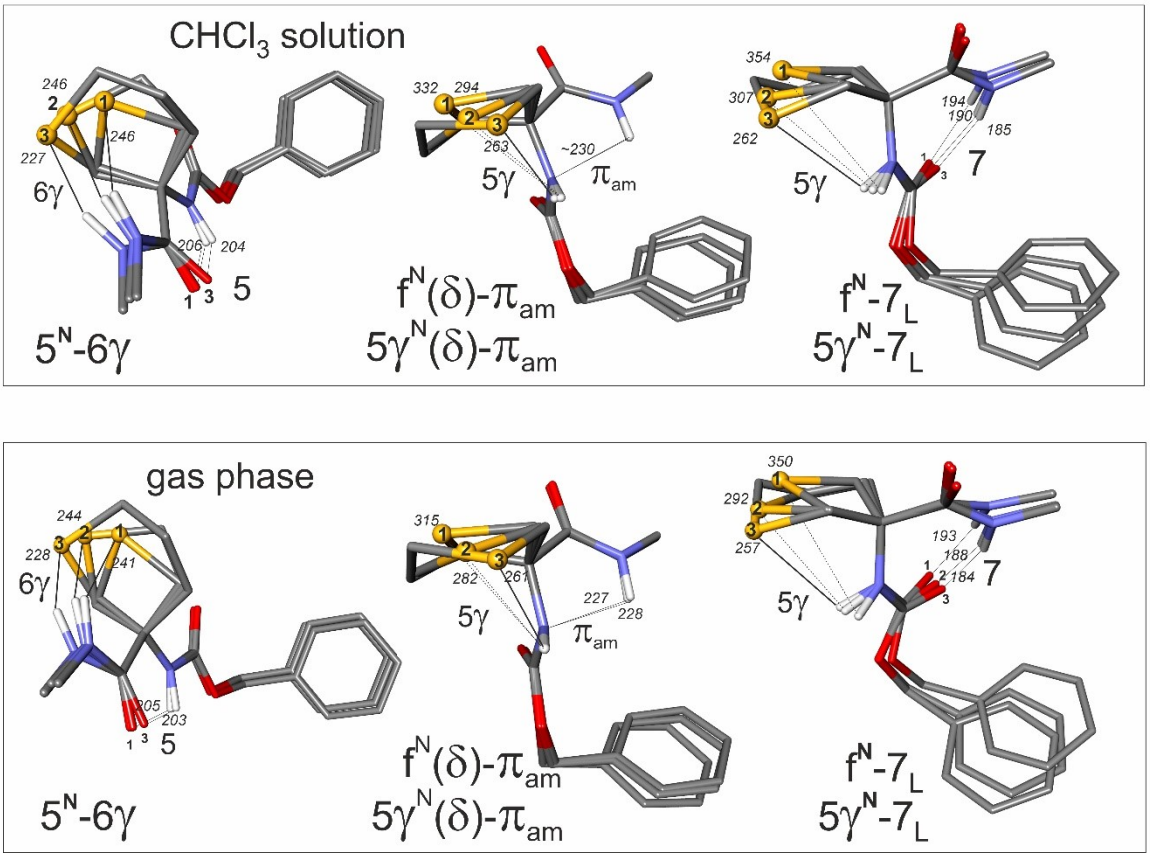

Figure S2.1. Comparison between calculated gas phase (*lower panel*) and chloroform solution (*upper panel*) structures for the several backbone families of compounds **1**-**3**, illustrated for the *S* configuration, with the *gauche+* rotamer of the C-terminus benzyl moiety and a *trans* carbamate. For the sake of structural comparison, the C1, Cα, and N2 atoms of each species have been overlapped. The H-bond NH···O/S/N distances are given in pm. The nomenclature indicates the status of the successive NHs' along the backbone, together with the ring puckering (N/O) and the configuration (L/D or δ/δ') of the chiral backbones.

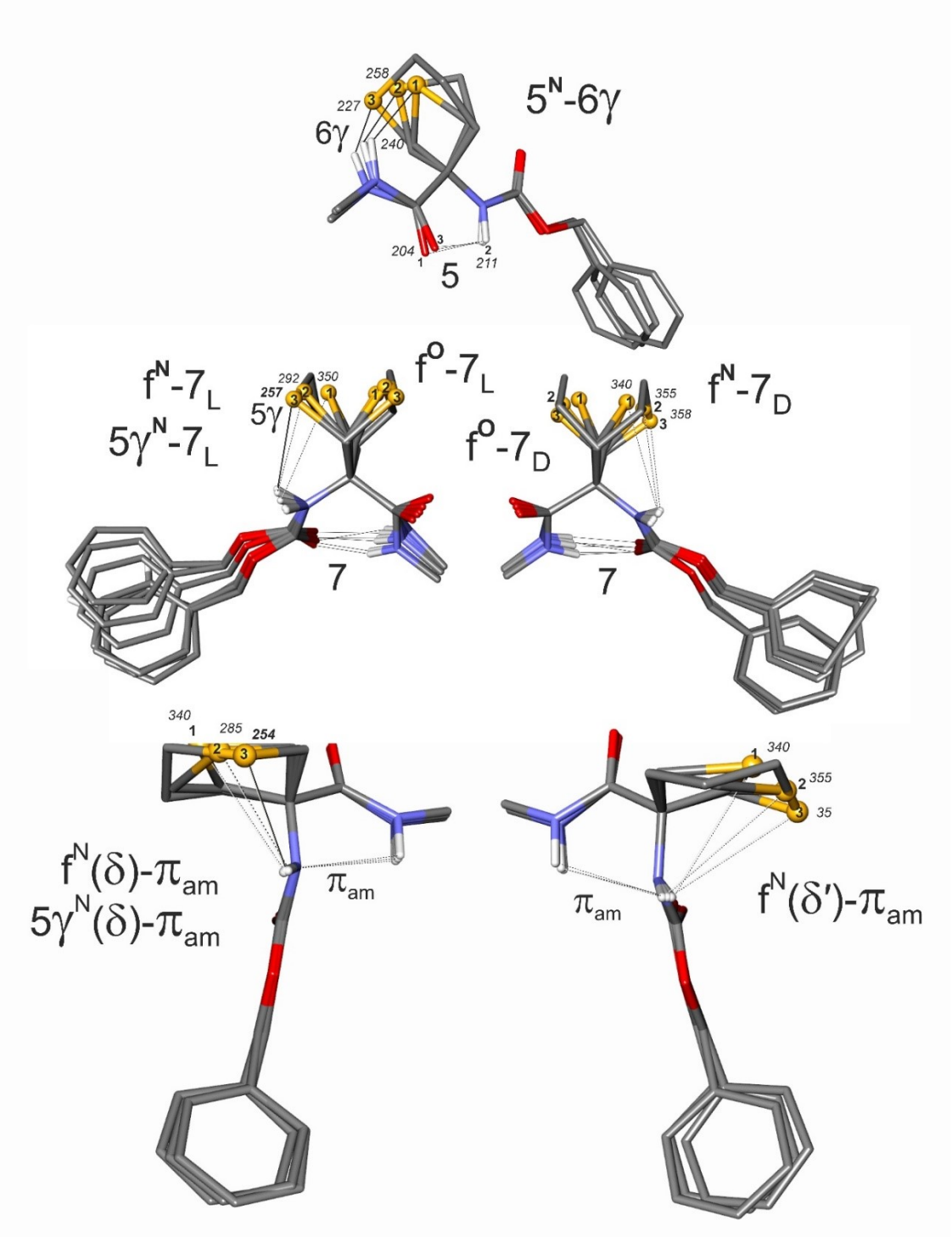

Figure S2.2. Gas phase calculated structures for the several backbone families of compounds **1**-**3**, illustrated with the *trans* rotamer of the C-terminus benzyl moiety and a *trans* carbamate. For the sake of structural comparison, the C1, Cα, and N2 atoms of each species have been overlaid. The H-bond NH···O/S/N distances are given in pm. The nomenclature indicates the status of the successive NHs' along the backbone, together with the ring puckering (N/O) and the configuration (L/D or δ/δ') of the chiral backbones.

S2.3 Conformational landscapes

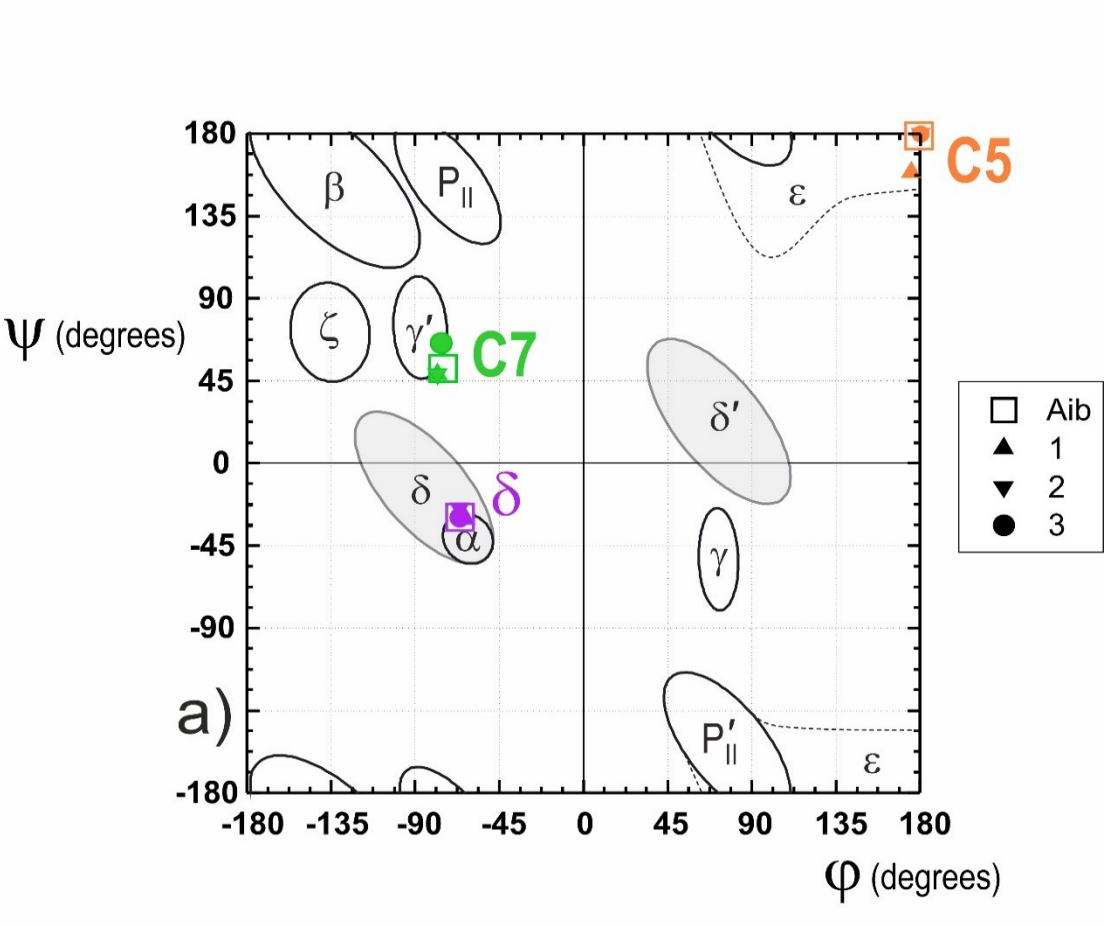

Figure S2.3. Backbone geometries of the three low energy backbone conformations (C5, C7 and δ) for compounds **1**-**3** on the classical Ramachandran map, together with their Aib counterpart compound (MeO-CO-Aib-NHMe), as obtained in solution at the DFT-D level of theory with a polarizable continuum model.

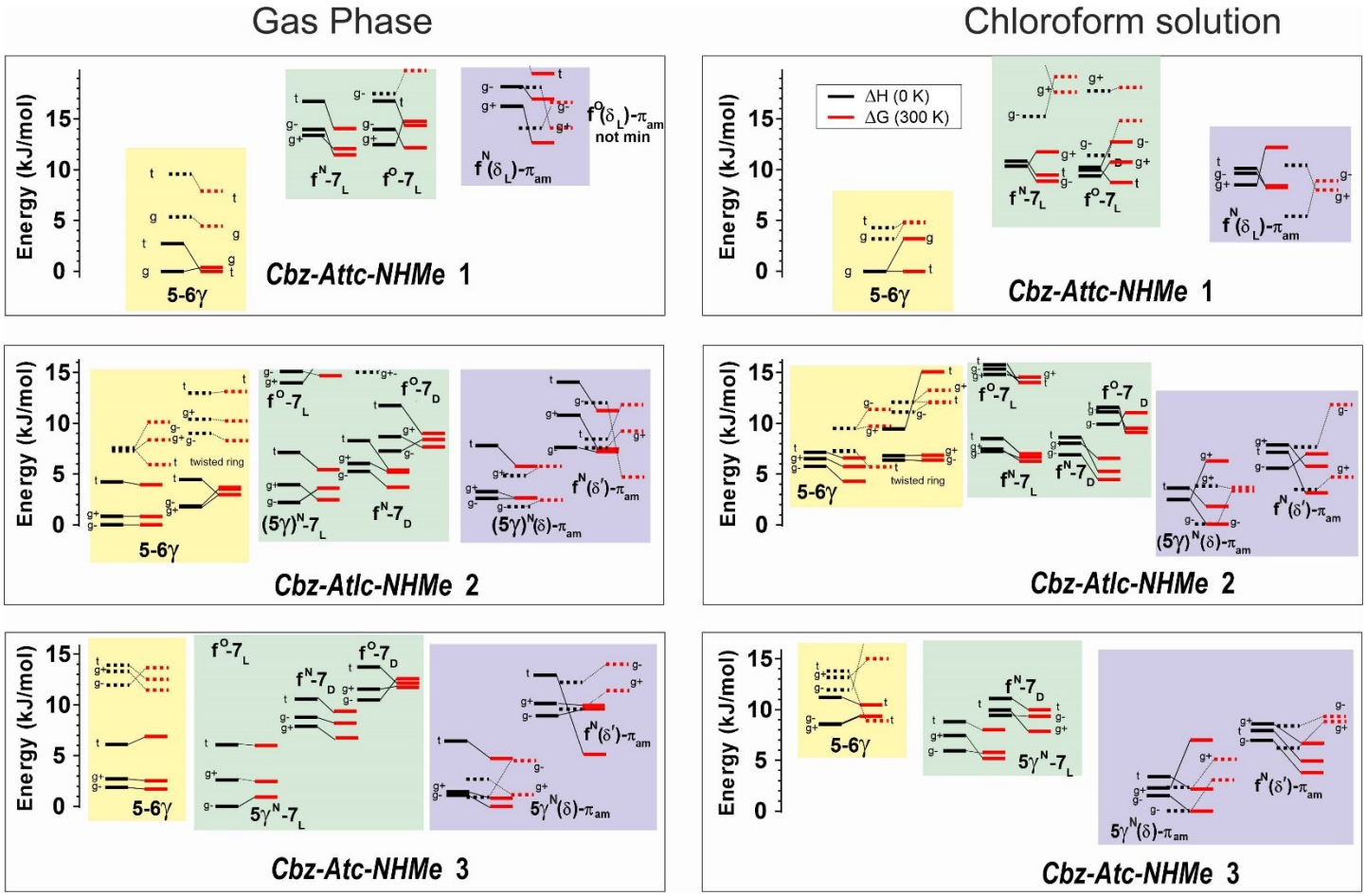

Figure S2.4. Comparison of the conformational landscapes of the *S* conformation of compounds **1**-**3** in the gas phase (left) and in chloroform solution (right). Stabilities are indicated at 0 K (in black) and 300 K (red). See Figs. 2, S1 and S2 for conformational nomenclature.

S3. Gas phase conformer-selective laser spectroscopy

Experimental characterization in the gas phase was carried out using IR spectroscopy. This technique was recently demonstrated to provide a precise diagnostic of the H-bonding network of amino acid derivatives.[1] The experimental set-up was described in detail previously.[24] Solid samples (pellets made of pressed mixtures of peptide and graphite powders) were first vaporized using laser-desorption (second harmonic of a Nd:YAG laser), bringing the isolated molecules to a high temperature. Interaction with a pulsed supersonic expansion (18 bar of a He:Ne mixture; nozzle diameter 1 mm) cooled them down rapidly, with two outcomes: on the one hand, freezing the interconversion between backbone families (which requires crossing of high energy barriers), leaving a conformational distribution described by a high temperature (typically room temperature[21, 24]); on the other hand, within each backbone family a rotational and vibrational cooling and funneling of the population to the most stable conformers occurs. Subsequently, conformer-selective laser methods[21, 24] enabled us to exquisitely characterize the structures detected in the expansion. Near-UV absorption spectra of the Cbz chromophore of compounds **1-3** were obtained through mass-selected resonant two-photon ionization in the interaction region of a time-of-flight mass spectrometer, following skimming of the supersonic expansion. The Cbz-cap UV spectroscopy being sensitive to the molecular conformation, the cooling finally achieved ensured the observation of narrow UV features in the origin region of the first $\pi\pi^*$ transition of the phenyl group (Figure S4), enabling us to assess the conformational populations. Then vibrationally-resolved conformer-selective IR spectra were recorded using the double-resonance IR/UV spectroscopic technique. Briefly, the UV laser (Continuum Nd:YAG-pumped Radiant NarrowScan dye laser) is fixed on one of the resolved features of the UV spectrum in order to probe selectively the ground state level of a certain conformer in the supersonic expansion. An IR laser (OPO/OPA, LaserVision), sent a few ns before the UV laser, is scanned in a spectral region of interest: principally the NH stretch range, but in some cases the amide I and II regions (generated in a difference frequency generation module). When the IR laser is tuned on an IR transition of the conformer probed, it causes a decrease of the ground state population, which is easily monitored as a depletion in the UV signal. The conformer-specific spectra thus obtained were then assigned by comparison with the theoretical IR spectra of low energy conformations, which thus provided a detailed description of the intramolecular H-bond content of each conformer.

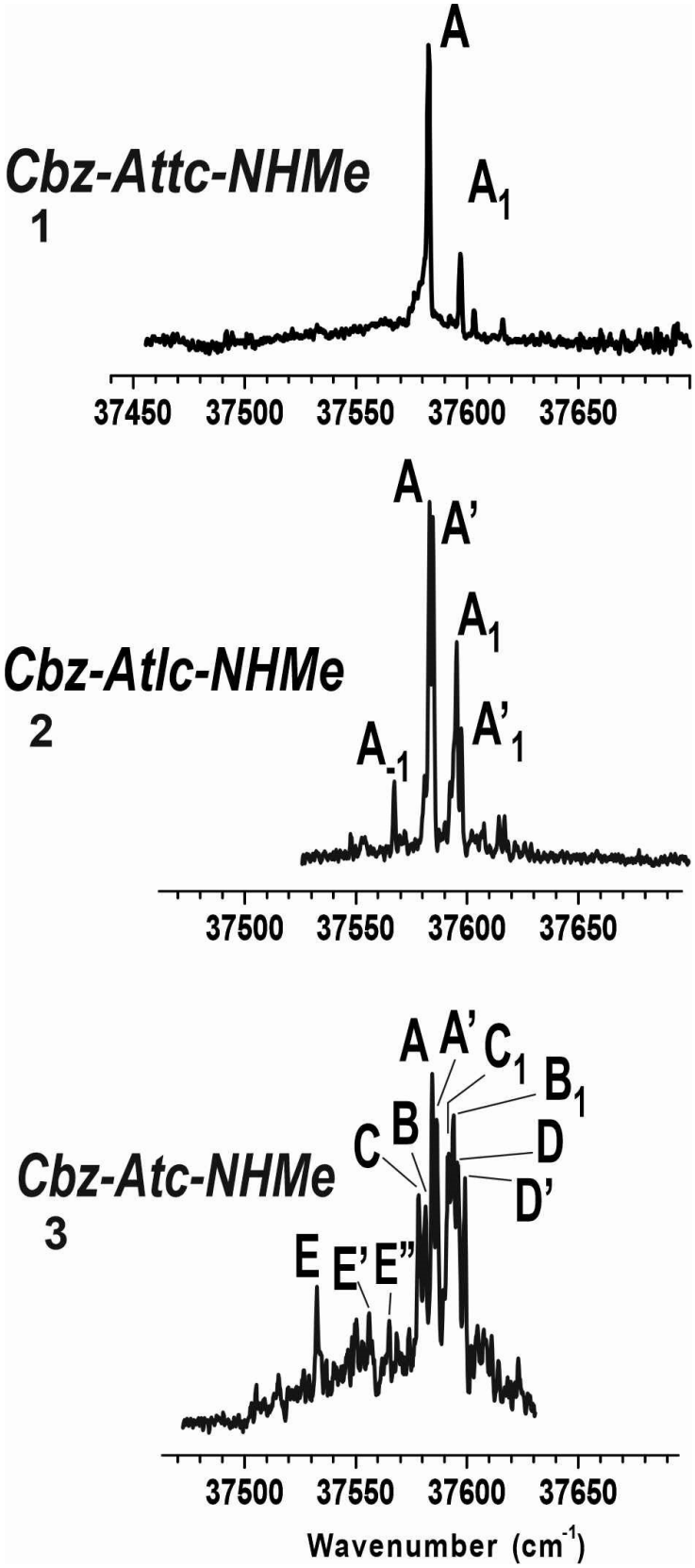

Figure S3. Near-UV spectra of compounds **1**-**3** as obtained from mass-selected resonant two-photon ionization spectroscopy, in the origin region of the first $\pi\pi^*$ transition of the phenyl ring. UV bands are labelled according to the IR/UV spectra recorded from them (see details below). A, A_1, A_{-1} bands belong to the same conformer; labels with and without prime indicate species characterized by similar IR/UV spectra (see next section), and are assigned to conformer sharing the same peptide backbone, *i.e.* differing only by the conformation of their Cbz-cap.

S4. IR spectroscopy in the gas phase

S4.1 Compound **2**

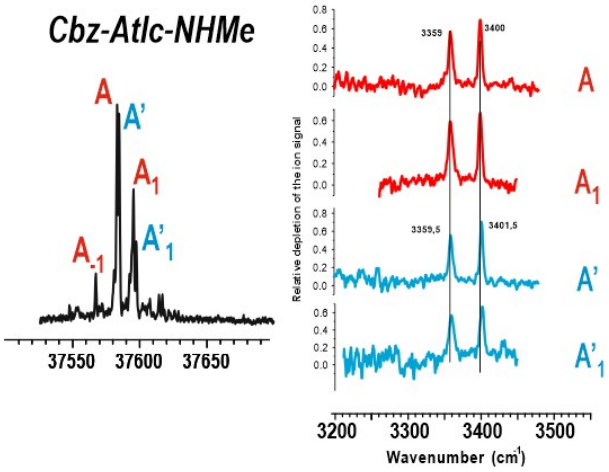

Figure S4.1. Experimental UV spectrum of **2** (*left panel*) and conformer-specific IR/UV spectra obtained by probing the UV transitions A, A_1 and A', A'_1 (*right panel*). The vertical guidelines provide evidence for slight differences between red and blue spectra and hence conformers sharing a same backbone conformation. The UV transition A_{-1} also give rise to depopulation on the same IR bands as A, showing that they belong to the same conformer. The absolute accuracy of the experimental IR frequency values is ± 2 cm^{-1}.

The NH stretch IR spectra of **2**, recorded by probing the conformational population on UV bands A and A_1 on the one hand, and A' and A'_1 on the other hand, showed very similar spectra (Figure **S4.1**), differing by only a few cm^{-1}. These band systems were thus assigned to two conformers differing only in the Cbz cap orientation: presumably two *gauche* orientations. Due to the presence of a chiral center, the *gauche+* and *gauche–* forms are no longer enantiomeric (in contrast with the Attc derivative **1**); their UV spectra were nonetheless expected to be similar due to the poor interactions between the Cbz terminal and the rest of the molecule. The IR spectrum (Figure 5 and S4.1) was composed of two narrow IR NH stretch features, one of them found in the 3400 cm^{-1} range and the second one further to the red (3359 cm^{-1}). It bore a great similarity with the spectrum of **1** (Figure 4). Its assignment to an extended conformer with a 5-6γ backbone (Figure 3), was supported by i) the highest stability of this backbone structure in the gas phase (Fig. 2), ii) the reasonable agreement with the theoretical IR spectra (with the same type of error on the strength of the NH···S bond, as previously reported on the derivatives of **1**), and iii) on the striking spectral similarities with **1**.

S4.2 Compound **3**

In contrast to **1** and **2**, the numerous UV features of **3** led to five different NH stretch IR spectra (labelled A-E), since several sets gave rise to undistinguishable spectra, namely (A, A'), (B, B1), (C, C1), (D, D') and (E, E1, E2) shown in Figure S4.2, suggesting their assignment to vibronic bands of the same conformer and/or to conformers differing only by the Cbz cap orientation.

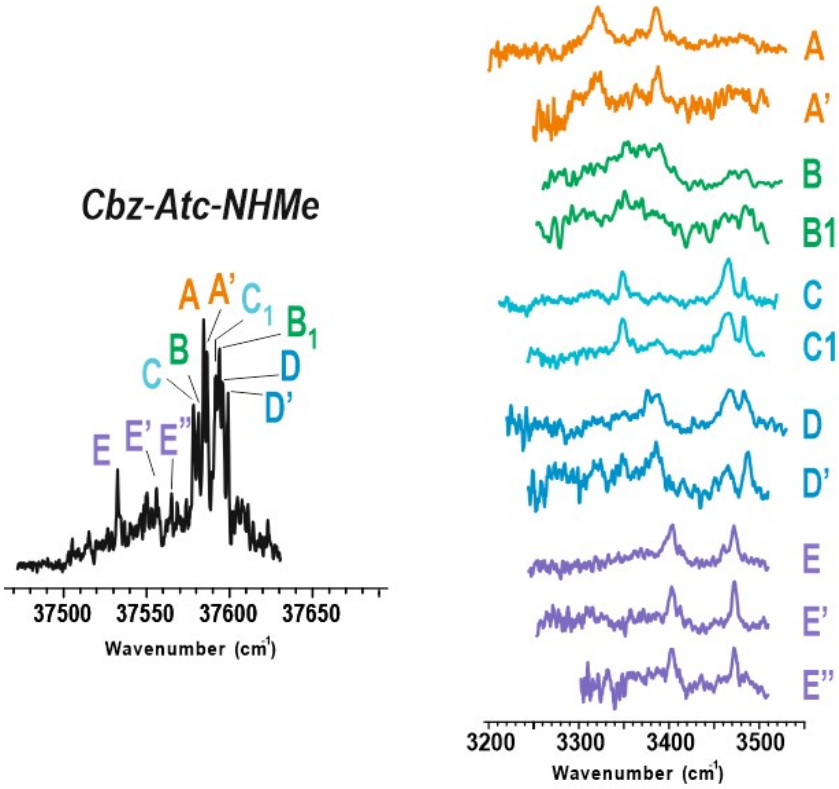

Figure S4.2. Experimental UV spectrum of **3** (*left panel*) and conformer-specific IR/UV spectra obtained by probing the UV transitions A-E" (*right panel*). The absolute accuracy of the experimental IR frequency values is ± 2 cm^{-1}.

Among the several spectra of **3**, that obtained on band A shared some similarity with that recorded for **2** (Figure S4.3), in particular a high frequency band, at 3386 cm^{-1}, in the NH stretch region recently identified as characteristic of a C5 band in α,α-disubstituted amino acids.[25] Theoretical spectra of the lowest extended or folded forms (5-6γ (*g*+) and 5γ-7_D (*g*+) respectively) showed a reasonable, although not perfect, match with experiment. However, the amide II spectrum (Figure S4.4), with the specific feature at 1480 cm^{-1}, well reproduced by theory, enabled us to assign A to a 5-6γ extended backbone structure, rather than to a γ-folded backbone. This is further supported by i) the spectral similarities with **2**, ii) the red shift overestimation of the 6γ band, observed so far at this level of theory in **1** and **2**, and iii) the presence of the A, A' doublet, easily assigned to the two *gauche* rotamers of the Cbz cap, as expected in a chiral species.

The bands C to E (red contour, Fig. S4.2) all shared a similar IR pattern, with one relatively blue feature (at ~3470 cm^{-1}), appearing as a doublet with some changes in the relative intensities of the components, and one red shifted band in the 3330-3400 cm^{-1} range. The first one, whose doublet structure was assigned to a Fermi resonance with the overtone of a CO stretch (Figure S4.4) at 1750 cm^{-1}, is characteristic of a free or nearly free NH. It was labelled π_{am} to recall the proximity of NH(2) to the first amide. The other band fitted a medium/weak range H-bond, consistent with a 5γ H-bond, as previously reported in related compounds.[22, 24]

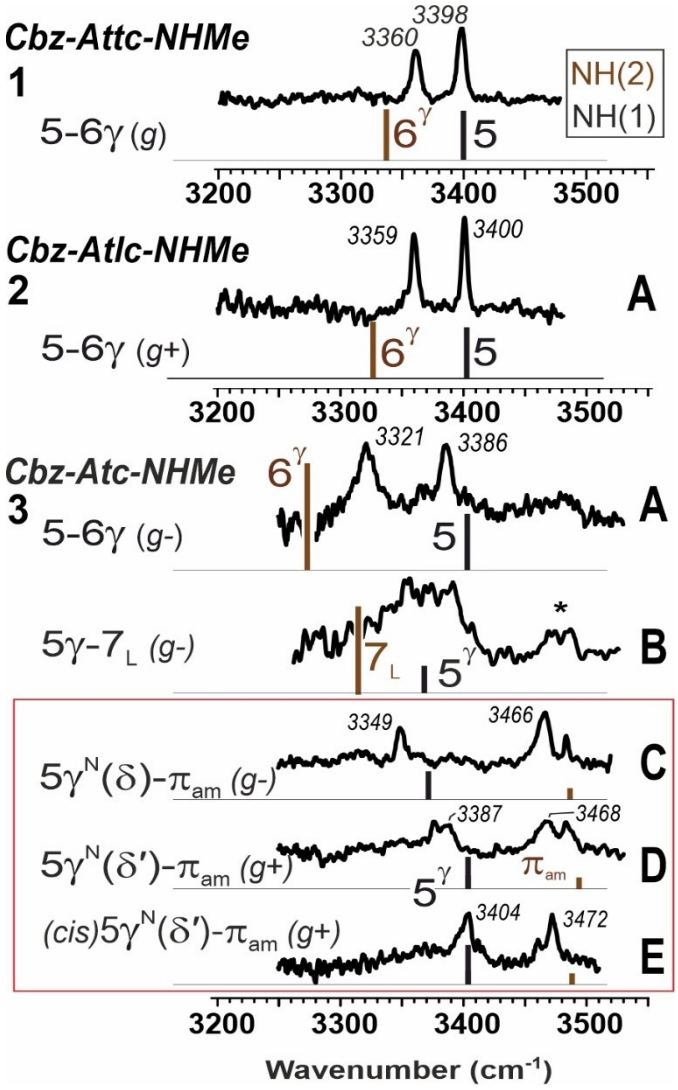

Figure S4.3. Gas-phase conformation-selective IR spectra (black), recorded by IR/UV double resonance method for compounds **1-3**: The letter labels (right) refer to the UV band used for conformer selection. The bands indicated with an asterisk in conformer B of **3** are an artefact arising from conformers C-E due to accidental overlaps in the UV spectra (see Fig. S4.2). For comparison, theoretical IR spectra (sticks) are given for selected representative low energy gas phase conformations. The IR spectrum of **1** is adapted from ref. 1.

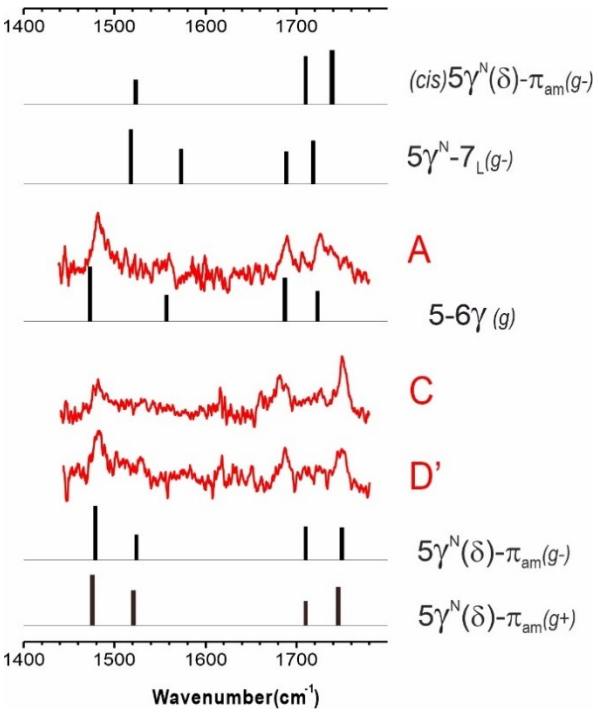

Figure S4.4. Experimental conformer-specific IR/UV spectra of compound **3** obtained by probing the UV transitions A, C and D', in the amide I and II regions, compared with low energy structures of the three backbone families (see Fig. S3). The absolute accuracy of the experimental IR frequency values is ± 3 cm^{-1}. The A bands better fit a 5-6γ conformer whereas bands C and D' are better reproduced by δ-folded forms.

Comparison of the spectra of C and D with theory provided a nice agreement with the lowest forms of a δ-folded 5γ-π_{am} backbone, with again different *gauche* Cbz rotamers. In this regard, one should expect, like in the A, A' UV doublet, similar and neighbouring UV patterns for the species C and D. Whereas C1 could confidently be assigned to a vibronic band, built on the C origin, this assignment did not fit the small frequency difference of D and D'. It may have been that the UV origin band of the D species was closer to that of C and remained undetected due to spectral congestion in this region. In this case bands D and D' would actually be vibronic bands. The IR spectrum of E was also well reproduced by a low energy conformation of a δ-folded backbone, with however a *cis* conformation of the N-terminus carbamate. The red-shifted UV bands E, E1 and E2 compared to other species supported this view, due to the sensitivity of the phenyl spectroscopy to the conformation of its carbamate neighbour.

Finally, two UV bands, B and B', located in a congested spectral region, exhibited a similar IR spectrum, which differed from the others, featuring a broad feature in the 3370 cm^{-1} region, accompanied with a weak doublet (marked with an asterisk in Figs. S4.2 and S4.3) in the 3470 cm^{-1} range; all these absorptions being also observed in the C-E spectra. This suggested that these spectra could arise from a simultaneous probe of species C-E, in agreement with the UV spectral congestion. However, the strength and breadth of the 3370 cm^{-1} IR band, the relative weakness of the blue side doublet and the appearance of the same spectrum on both bands B and B' suggests that it originates from another species. A fair agreement is met with the theoretical spectrum of the lowest conformation of a 5γ-7 folded backbone, suggesting us to propose such a structure for B.

S5. IR spectroscopy in solution

Solution state infrared spectra of compounds **1-3** were recorded in $CHCl_3$ on a Fourier-transform Perkin Elmer Spectrum Two spectrometer; solutions were held at 293 K in Omni-cell Specac 1 mm path-length NaCl plates. Figure S5.1 shows the superposition of the absorbance bands in the NH stretch (amide A) region for a 5 mM solution of each compound. Figure S5.2 shows the superposition of the NH stretch bands at three different concentrations (5 mM, 10 mM, 30 mM) for each of the three compounds.

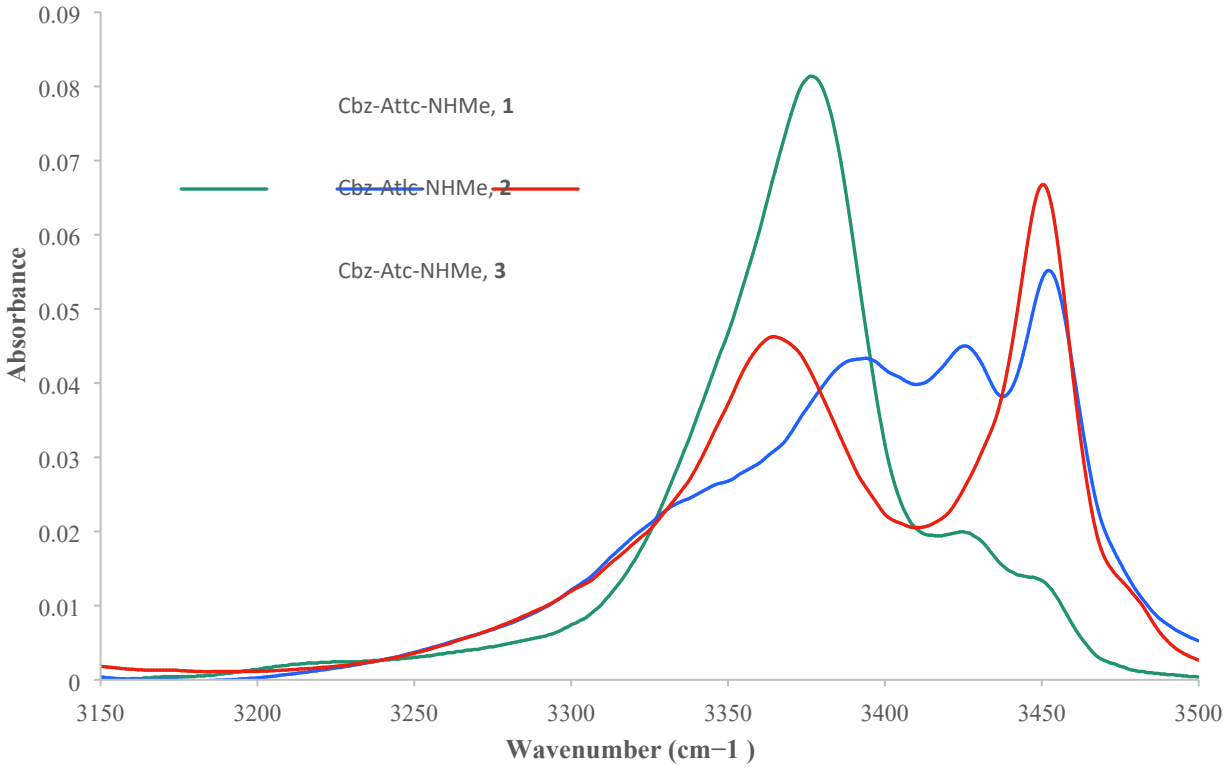

Figure S5.1. Solution state IR absorption spectra of compounds **1**-**3** in the NH stretch region (5 mM in chloroform).

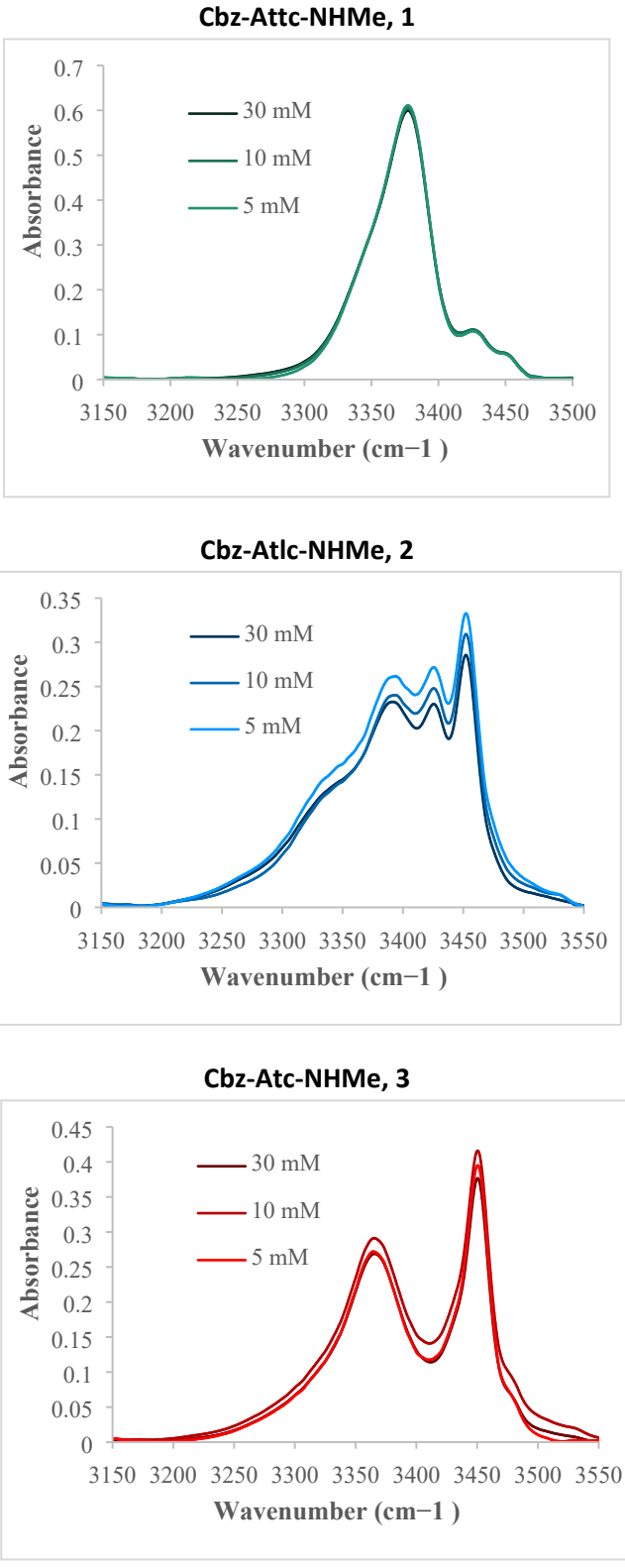

Figure S5.2. Solution state IR absorption spectra of each compound **1**-**3** in the NH stretch region at three different concentrations.

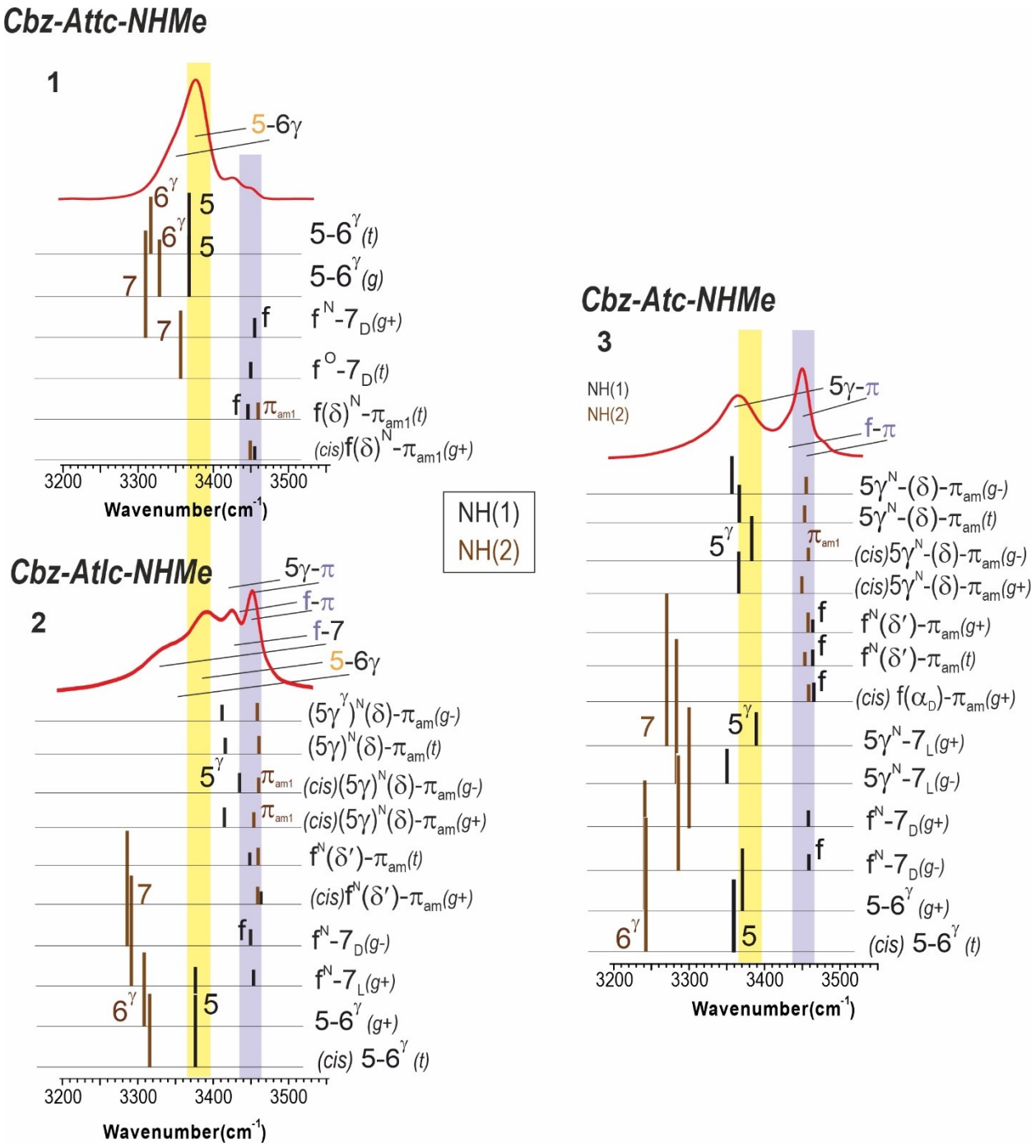

Figure S5.3. Solution state IR spectra of compounds **1**-**3** (5 mM in chloroform) and the calculated IR spectra in solution of the most energetically relevant conformations for each backbone family. The colored zones indicate the typical locations of diagnostic spectral features: nearly free (π_{am}) NH in a δ backbone (violet) and NH engaged in a C5 H-bond (yellow).

S6. NMR studies of compound 3 in solution

S6.1 DMSO-d_6 titration

^{1}H NMR spectra were recorded at 300 K on a Bruker spectrometer operating at 400 MHz. The sample of compound **3** was dissolved in $CDCl_3$ (400 µL) to give a 5 mM solution for which the 'starting point' spectrum was recorded. Aliquots of DMSO-d_6 were added successively to the NMR tube and each addition was followed by rapid agitation then re-recording of the ^{1}H spectra. Data are presented in Fig. S6.1.
Over the range of 10% added DMSO-d_6, values of $\Delta\delta$ above 0.5 are considered to indicate conformational mobility due to solvent accessibility.[26] The low values observed here for **3** are in agreement with both NH protons being only weakly influenced by the solvent, compatible with a folded conformational bias such as that of the π_{am} interaction of the δ conformation.

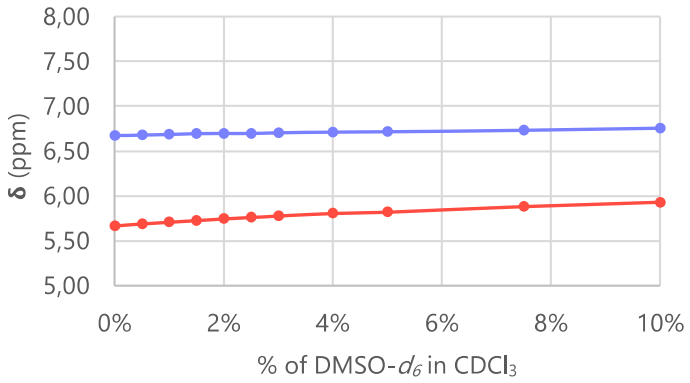

NH	Δδ (for 10% of DMSO-d_6)
NH^2	0,08
NH^1	0,26

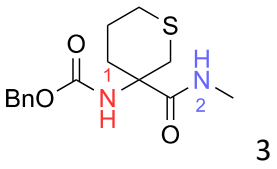

3

Figure S6.1. ^{1}H NMR DMSO-d_6 titration curve for compound **3.**

S6.2 NOESY experiment

A NOESY experiment was performed on compound **3** (20 mM solution in $CDCl_3$). Data were acquired at 273 K on a Bruker spectrometer operating at 600 MHz. The pulse sequence was noesygpph, and the mixing time was 600 ms. The experiment was performed by collecting 1024 points in f2 and 512 points in f1. The correlations between NH atoms and aliphatic CH atoms are shown in Fig. S6.2. Illustrations of these correlations and the corresponding interatomic distances expected in the C5-C6γ conformer of **3** [from Fig. S2.1; chloroform solution panel; labelled $5\gamma^{N}(\delta)$-π_{am}] are presented in Table S6.1, showing good compatibility of the experimental data with the expected behaviour of the δ conformation.

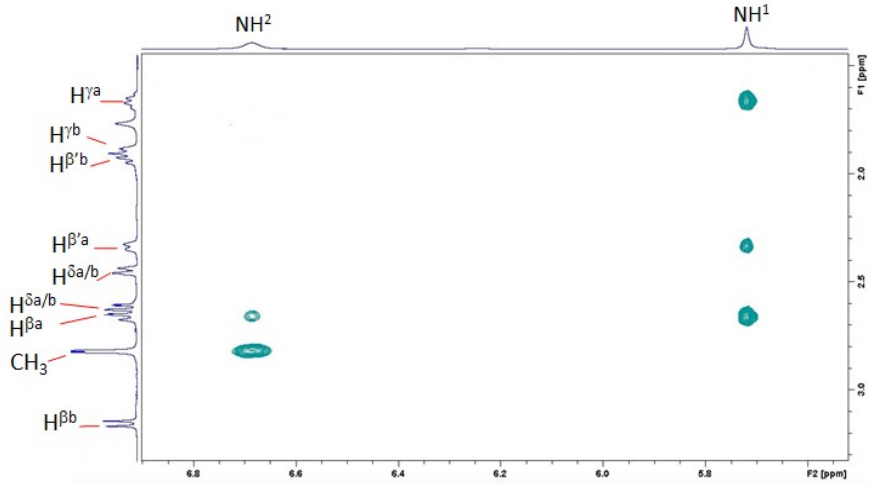

Figure S6.2. NOESY correlation plot

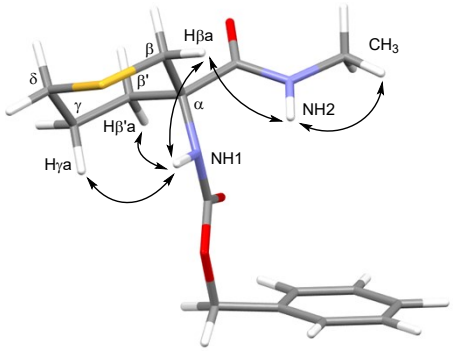

Table S6.1. NOESY correlation data

NH	NOE correlation	Strength of NOE	Interatomic distance (Å)
NH^1	$H^{\gamma a}$	strong	2.90
	$H^{\beta' a}$	medium	3.50
	$H^{\beta a}$	strong	2.65
NH^2	$H^{\beta a}$	medium	2.90
	CH_3	strong	2.32

S7. References

[1] Z. Imani, V. R. Mundlapati, G. Goldsztejn, V. Brenner, E. Gloaguen, R. Guillot, J.-P. Baltaze, K. Le Barbu-Debus, S. Robin, A. Zehnacker, M. Mons and D. J. Aitken, *Chem. Sci.*, 2020, **11**, 9191-9197.

[2] M. Hatanaka and T. Ishimaru, *Bull. Chem. Soc. Jpn.*, 1973, **46**, 2515-2519.

[3] M. Oba, A. Shimabukuro, M. Ono, M. Doi and M. Tanaka, *Tetrahedron: Asymmetry*, 2013, **24**, 464-467.

[4] K. Lavrador, D. Guillerm and G. Guillerm, *Bioorg. Med. Chem. Lett.*, 1998, **8**, 1629-1634.

[5] J. Hamon, F. Espaze, J. Vignon and J. M. Kamenka, *Eur. J. Med. Chem.*, 1999, **34**, 125-135.

[6] P. G. McCaw, N. M. Buckley, K. S. Eccles, S. E. Lawrence, A. R. Maguire and S. G. Callins, *J. Org. Chem.*, 2017, **82**, 3666-3679.

[7] D. E. Ward, M. A. Rasheed, H. M. Gillis, G. E. Beye, V. Jheengut and G. T. Achonduh, *Synthesis*, 2007, 1584-1586.

[8] B. Unterhalt and A. Scheppan, *Sci. Pharm.* , 2001, **69**, 271-274.

[9] G. R. Fosker and W. Davies, 1972, Pat. DE 2215721.

[10] R. Gomez, J. Ding, R. M. Oballa, D. A. Powell and M. Epifanov, 2017, Pat. WO 2017222915.

[11] A. P. Kozikowski and A. H. Fauq, *Synlett*, 1991, 783-784.

[12] Macromodel, 2019, Release 2019-2013 ; Schrödinger, LLC, New York, NY.

[13] Turbomole V7.2, 2017, a development of University of Karlsruhe and Forschungszentrum Karlsruhe GmbH, 1989-2007, Turbomole GmbH, since 2007; available from http://www.turbomole.com.:

[14] S. Grimme, S. Ehrlich and L. Goerigk, *J. Comput. Chem.*, 2011, **32**, 1456-1465.

[15] D. Rappoport and F. Furche, *J. Chem. Phys.*, 2010, **133**, 134105.

[16] A. Schafer, C. Huber and R. Ahlrichs, *J. Chem. Phys.*, 1994, **100**, 5829-5835.

[17] M. Sierka, A. Hogekamp and R. Ahlrichs, *J. Chem. Phys.*, 2003, **118**, 9136-9148.

[18] K. Eichkorn, O. Treutler, H. Ohm, M. Haser and R. Ahlrichs, *Chem. Phys. Lett.*, 1995, **242**, 652-660.

[19] K. Eichkorn, O. Treutler, H. Ohm, M. Haser and R. Ahlrichs, *Chem. Phys. Lett.*, 1995, **240**, 283-289.

[20] K. Eichkorn, F. Weigend, O. Treutler and R. Ahlrichs, *Theor. Chem. Acc.*, 1997, **97**, 119-124.

[21] E. Gloaguen, M. Mons, K. Schwing and M. Gerhards, *Chem. Rev.*, 2020, **120**, 12490-12562.

[22] G. Goldsztejn, V. R. Mundlapati, V. Brenner, E. Gloaguen, M. Mons, C. Cabezas, I. Leon and J. L. Alonso, *Phys. Chem. Chem. Phys.*, 2020, **22**, 20284-20294.

[23] A. Klamt and G. Schuurmann, *J. Chem. Soc., Perkin Trans. 2*, 1993, 799-805.

[24] V. R. Mundlapati, Z. Imani, G. Goldsztejn, E. Gloaguen, V. Brenner, K. Le Barbu-Debus, A. Zehnacker-Rentien, J.-P. Baltaze, S. Robin, M. Mons and D. J. Aitken, *Amino Acids*, 2021, **53**, 621-633.

[25] V. R. Mundlapati, Z. Imani, V. C. D'mello, V. Brenner, E. Gloaguen, J.-P. Baltaze, S. Robin, M. Mons and D. J. Aitken, *Chem. Sci.*, 2021, **12**, 14826-14832.

[26] H. Awada, C. M. Grison, F. Charnay-Pouget, J.-P. Baltaze, F. Brisset, R. Guillot, S. Robin, A. Hachem, N. Jaber, D. Naoufal, O. Yazbeck and D. J. Aitken, *J. Org. Chem.,* 2017, **82**, 4819-4828.